CHARACTERIZATION OF AGROFORESTRY FEEDSTOCKS AND THEIR BIOCHARS AND THEIR EFFECTS ON SOIL GREENHOUSE GAS EMISSIONS IN A FLOODPLAIN SOIL

A Thesis

presented to

the Faculty of the Graduate School

at the University of Missouri-Columbia

In Partial Fulfillment

of the Requirements for the Degree

Master of Science

---

by

BOAZ K. BETT

Dr. Peter Motavalli, Thesis Co-Supervisor

Dr. Manjula Nathan, Thesis Co-Supervisor

DECEMBER 2018

The undersigned, appointed by the dean of the Graduate School, have examined the thesis entitled

CHARACTERIZATION OF AGROFORESTRY FEEDSTOCKS AND THEIR BIOCHARS AND THEIR EFFECTS ON SOIL GREENHOUSE GAS EMISSIONS IN A FLOODPLAIN SOIL

presented by Boaz K. Bett,

a candidate for the degree of master of science,

and hereby certify that, in their opinion, it is worthy of acceptance.

Dr. Peter Motavalli

Dr. Manjula Nathan

Dr. Chung-Ho Lin

ACKNOWLEDGEMENTS

I would like to acknowledge my advisor Dr. Peter Motavalli for providing me the excellent opportunity of being his graduate research assistant. During the duration of this position he has graciously offered me his wisdom to develop my professional skills. His influence has impacted me and will undoubtedly follow me as I continue into my future endeavors. This research project was only possible because of his enthusiasm to spend time to develop the research from an idea and management of all the logistics leading up to the completion of this project.

I would like to express my gratitude to my co-advisor Dr. Manjula Nathan for providing me with not-only key funding and an opportunity to use her soils lab equipment, but also guidance and support during my master's research, allowing me to gain experience in soils testing procedures.

I am grateful to Dr. Shibu Jose for providing me with additional funding from the Center for Agroforestry, which allowed me to expand my research focus and to include agroforestry feedstock from HARC in my biochar studies.

I thank Dr. William Jacoby for supporting my research by allowing me access to his research lab and biochar reactor at the Agricultural Engineering department. I also thank Dr. Keith Goyne for providing me with guidance and access to his FTIR spectrometer, and for sitting on my thesis committee for most of my master's career, and I wish him well in his new appointment at Virginia Tech.

I would like to extend my humble gratitude to Dr. Chung Ho Lin for not-only accepting to replace Dr. Goyne's seat on my thesis committee, but also for offering encouragement on my research during my master's program.

I would like to also extend my sincere gratitude to Patricia Quackenbush for providing me with teaching assistantships and for not only-trusting me with her students, but also giving me an opportunity to develop my skills in teaching. Her wisdom and vast knowledge have been a source of strength and encouragement to me.

I would also like to thank Dr. Kristen Veum for helping me conduct C/N analyses of my feedstock and biochars, which provided important data sets that contributed to the success of this research possible.

I would also like to show my appreciation to Nictor Namoi, whose visit to the University of Missouri form ICRAF was a timely solution as he offered his excellent Statistical Analytical skillset in relation to this research project; he has also sparked my interest in data analysis. I would also like to thank Tyler Steusloff for not-only being a friend and colleague, but for helping me with the labor-intensive sampling of headspace gases.

I would like to express my gratitude to my family, beginning with my beloved wife Judy C. Bett, and my loving daughter Bethel C. Bett, without whom I would have completed this thesis long ago, yet with whom my endeavor gained supreme meaning. If it wasn't for their tireless support, perseverance and prayer, it would have been difficult to achieve results. Brother Pavel Bosovik, his wife Nina Bosovik and their family have been of great and significant support to me throughout this journey as well, and I thank them sincerely. My brother Dominic Bett, sister Abigael Kosgei, parents Wilson and Esther and my siblings have been patient with me and I am grateful to them. I would also like to thank Pr. Dempsey Collins and his wife Deena, Mr. Terrence Proctor and his wife Pamela, Dr. Craig Roberts and his wife Joetta, Mr. Paul Smith and his wife Lisa, and the entire Eastside Family who welcomed me among them and inquired about my progress.

I also would like to thank Mr. Andrew Etzler, my First Line Manager at the Columbia IBM Client Innovation Center for being gracious and accommodating my academic and research schedule, creating a seamless and work-school balance, as well as Baasandorj Namnansuren for mentoring me to succeed in my chosen career path. Finally, and most importantly, I thank God in whom I live, move and have my being and who gave me strength, and in whose hands is the course of my life.

TABLE OF CONTENTS

LIST OF TABLES

LIST OF FIGURES

Figure **Page**

CHAPTER 1

LITERATURE REVIEW

Biochar (or biocharcoal) is a fine-grained, highly porous charcoal produced through pyrolysis or gasification. To produce biochar using these processes, feedstock is heated at high temperature in the absence (or under reduction) of oxygen to produce a carbonaceous material that resists degradation when applied to soil (International Biochar Initiative, 2017). Hydrochar, on the other hand, is a hydrophobic form of biochar produced during the hydrothermal carbonization (HTC) process, which involves the use of compressed H_2O, typically at 200-275^oC and zero oxygen.

Biochar comprises part of a continuum of black carbon materials (i.e., soot, charcoal, and char) that are difficult to quantify (Schmidt et al., 2001). Biocharcoal has been extensively researched as an effective soil amendment to improve soil properties for crop growth and to sequester carbon to lower soil carbon dioxide emissions into the atmosphere (Lal et al., 2007; Laird et al., 2009; Spokas et al., 2010). Due to these beneficial effects of biochar amendments and the relatively inexpensive process of preparing biochar from a variety of feedstock, it has the potential to provide an additional source of revenue for small-scale producers utilizing agroforestry practices (Lal et al., 2007; Magdoff et al., 2009; Sohi et al., 2010).

There are seven preliminary properties that must be considered to evaluate biochar (Kuwagaki, 1990). These properties include pH, volatile compound content, ash content, water holding capacity, bulk density, pore volume, and specific surface area. Of the governing factors for biochar properties (e.g., feedstock type, temperature, O_2 amount, particle size, pyrolysis time), pyrolysis temperature is arguably the most significant process parameter that determines biochar yield in its production through

pyrolysis, physical and chemical qualities, such as particle size, water-holding capacity and ash content.

Biochars are effective agents for soil C sequestration. Low-temperature biochars are generally more stable in soils than C in the original feedstock. The organic C in moderate- and high temperature biochars is stabilized against microbial decomposition and may persist in soils for hundreds if not thousands of years (Sohi et al., 2010; Spokas et al., 2010). However, the net greenhouse gas (GHG) impact due to biochar applications to soil is also influenced by changes in the efficiency of residue mineralization or humification, soil organic matter cycling, and emissions of CO_2, CH_4 and N_2O (Larson et al., 2009; Sohi et al., 2010; Jeffery et al., 2011; Jeffery et al., 2013). Furthermore, the overall impact of biochar amendments on GHG emissions must also include GHG emissions resulting from biochar production, transport, and soil application.

According to findings by Yoo and Kang (2012) in a study examining the effects of adding biochar and swine manure mix to two different soils, the N-limited soil released less CO_2 and CH_4 with biochar containing elevated available N (i.e., swine manure biochar). However, the reduced soil CO_2 and CH_4 emissions observed in the study were likely offset by increased soil N_2O emissions. In the same study, soil GHG emissions were also not increased when barley (*Hordeum vulgare*) stover biochar was added to either soil. Thus, it is suggested in the Yoo and Kang (2012) study that these types of biochar may be an appropriate amendment material to limit soil GHG emissions.

Kammann et al. (2012) conducted several laboratory incubation studies to investigate the effect of peanut hull biochars (produced between 500 and 800°C) in the absence or presence of organic amendments or fertilizer on soil GHG emissions. It was found that all biochar amendment scenarios exhibited significant reductions in soil N_2O

emissions except for the treatments that combined long-term elevated soil water contents and inorganic N fertilizer amendments. Biochar applications caused equal or less emissions of CO_2, N_2O, and CH_4 compared with control soils. Also, hydrochar applications caused larger releases of CO_2, N_2O, and CH_4 compared with the biochars and thus may not be a suitable material if soil C sequestration is a goal.

Augustenborg et al. (2012) applied either peanut hull (500°C) or Miscanthus (550°C) biochar to low- or high-organic matter soils, with or without endogeic (i.e., soil feeding) earthworms, and measured soil N_2O and CO_2 emissions. The authors found that biochar additions significantly reduced both CO_2 and N_2O emissions in the absence of earthworms compared with no-biochar controls. The endogeic earthworms increased soil N_2O emissions coming from the controls by as much as 12.6-fold; however, both biochars drastically reduced soil N_2O emissions in the presence of earthworms.

Yoo and Kang (2012) and Kammann et al. (2012) both found that biochar produced at higher pyrolysis temperatures caused a greater reduction in cumulative soil CO_2 release compared with biochars produced at lower temperatures.

Over a 365-day period, Qayyum et al. (2012) measured cumulative CO_2 released from three soils amended with either nothing, wheat straw, hydrochar (200°C), low-temperature biochar (sewage sludge pyrolyzed at 400°C), or charcoal (550°C). Cumulative soil CO_2 emissions generally followed the order: wheat straw > hydrochars > low temperature biochar > charcoal = control. The authors concluded that the biochar utilized for an application should match the aim of the use, with high-temperature biochars being good for soil C sequestration and low-temperature biochars perhaps better for enhancing soil fertility. These results agree with that of Brewer et al. (2012), which showed that biochar-amended soil CO_2 losses are inversely related to the extent of

pyrolysis. These studies illustrate that biochar type, pyrolysis conditions, and environmental factors all play a role in GHG emissions from biochar-amended soils.

Recent research has been conducted to understand the mechanisms and interactions among biochars, soils, and climate, as well as their impact on soil GHG emissions (Glaser et al., 2000; Glaser et al., 2001; Kammann et al., 2011; Jeffery et al., 2013). Short-term laboratory incubations are useful for screening biochars leading to guidelines for longer-term use; however, long-term field research should be done to quantify the effects of these interactions on net GHG emissions from agricultural soils (Spokas et al., 2010; Jeffery et al., 2011).

Analytical Determination of Biochar Properties

Scanning Electron Microscopy (SEM) is one of several techniques that can be used to provide a visual description of the physical structure of biochar, whose macroporous structure has effects on its water-holding and adsorption capacities (Day et al., 2005; Ogawa et al., 2006; Yu et al., 2006). Another analytical procedure is BET-N_2 analysis, which utilizes the Brunauer–Emmett–Teller (BET) theory to measure the surface area of materials by gas adsorption. The process temperature at which biochar is prepared is the driving factor governing surface area; $120 m^2 g^{-1}$ at 400^oC to $460 m^2 g^{-1}$ at 900^oC (Day et al., 2005). High pyrolysis temperature has been observed to produce results in which biochars possess characteristics analogous to activated carbon (Ogawa et al., 2006). The surface of low-temperature biochar is hydrophobic, limiting its water-storing capacity when it is added to soil. The type of feedstock subjected to pyrolysis affects quality and potential use of biochar, and biochar created at low temperature may be suitable for controlling the release of fertilizer nutrients (Day et al., 2005). High-temperature biochars are ideal for use as activated carbon (Ogawa et al., 2006).

The question as to whether bonding surface of low-temperature biochars with hydrophobic organic functional groups would be a viable endeavor to study still exists. The ratio of the exposed to total surface area is affected by particle size. Low-temperature biochar is stronger, but brittle and can abrade into smaller/finer fractions upon incorporation. Additional characterization techniques that have been elucidated (Baldock et al., 2002; Fernandes et al., 2003b; Lehmann et al., 2005b) include extractive techniques analogous to those applied to soil organic matter, solid-state 13-C NMR Spectroscopy with cross-polarization, CP, or Block Decay, combined with magic angle spinning (MAS), Diffuse Reflectance Infrared Fourier Transform Spectroscopy (DRIFT), and Near-edge X-Ray Absorption Structure (NEXAFS) Spectroscopy.

The key problem to characterization and quantification of biochar largely stems from interference from mineral matrix chemically resembling char. The employment of chemical oxidation methods with hydrofluoric acid to remove mineral interferences, a wet method developed by Simpson and Hatcher et al. (2004a), is one of the approaches utilized to characterize and quantify biochars. Newer methods involved chemically extracted and purified biomarkers, which include benzene polycarboxylic acid, BPCA (Brodowski et al., 2005) and Levoglucosan (Kuo et al., 2008). Other chemical oxidative treatments suggested involve acid dichromate/sodium chlorite treatment. Ultraviolet treatment (photo-oxidation) with correction for non-black aromatic carbon through 13-C NMR analysis of oxidized residues, the chemothermal oxidation method; using a temperature threshold of 375^{o}C, with ^{13}C NMR and elemental analysis of residues (Skjemstad et al., 1999; Smernik et al., 2002) can be used to characterize biochars *in situ* although these methods have been found to be inefficient (Oades, 2000 and Smernik et al., 2000). Methods used to rapidly estimate the quantity of carbon in the biochar include

thermogravimetric analysis using He-gas flow with 20% O_2 (Hammes et al., 2007; De la Rosa et al., 2008) and spectroscopic methods including thermal/optical laser transmittance and reflectance such as mid-infrared (Janik et al., 2007). It is applied to large sample sets (Lehmann et al., 2008) as a corrective technique calibrated against a reference method. Furthermore, matrix-assisted laser desorption ionization, MALDI-TOF (Bourke et al., 2007) with hydrogen pyrolysis (HyPy) for removal of black carbon (Ascough et al., 2009) is a method that involved analyses to identify feedstock source from the character of the diverse gaseous products of pyrolysis. The use of hydrofluoric acid (HF) for pretreatment to mitigate mineral interference (Simpson and Hatcher, 2004) and the use of pyrolysis gas chromatography mass spectrometry (PyGC/MS) and 13-C NMR spec with cross-polarization, Bloch decay and magic angle spinning, MAS (Skjemstad et al., 1999; Smernik et al., 2002) comprise a methodology that when combined, results in a much more effective method to secure more reliable results when discerning the physical and the chemical characteristics of biochars.

Mid-Infrared (MIR) Spectroscopy

Algorithms are available relating MIR response spectrum to black carbon, using a calibration set assessed based on a UV-oxidation method (Janik et al., 2007). These approaches have been used by Lehmann et al., (2008) to evaluate charcoal content in archived soils. They hold potential for assessments in the global context as algorithms that can be used for contrasting organic carbon contents. (Liang et al., 2006; Solomon et al., 2007; Sohi et al., 2009).

Raman Spectroscopy and FTIR

Raman Spectroscopy and FTIR are analytical techniques used to evaluate the chemical properties of biochar to provide the crystallite size distribution approximation

from the intensities of the D and G bands (Cancado et al., 2007), while Dispersive Raman spectroscopy has been utilized to examine the carbon nanostructure in biochar. The FTIR spectroscopy of biochar provides information regarding the relative contribution of chemical functional groups (Sohi 2010; Spokas 2010). It gives a qualitative indication of the aromaticity of samples.

The FTIR method has been used to determine the impact of pyrolysis temperature on the chemical composition of biochar. Increased pyrolysis temperatures lead to decreased C-O, O-H and aliphatic C-H intensities. (Solomon et al., 2007b); The *Terra Preta de Indio* soils were evaluated using specular reflection (SR) and attenuated total reflection (ATR)-FTIR spectroscopy to compare the content of phenolics, aliphatics, aromatics, carboxyls, and polysaccharides. Analysis of functional groups in *Terra Preta de Indio* soils showed elevated levels of recalcitrant carbon (aliphatic and aromatic) and increased carbon sequestration within these soils.

Research Objectives:

Objective 1: To determine the effects of feedstock type and laboratory preparation of biochars at 300^{o}C and 500^{o}C pyrolysis temperatures for highest solid particle biochar yields using FTIR-DRIFTS, NMR and other methodologies.

Hypothesis 1a: Slow pyrolysis, characterized by lower heating rates results in maximum solid product or biochar yields while fast pyrolysis, which involves high heating rates andlow vapor residence times, decreases the biochar yields, but enriches the biochar carbon content.

Hypothesis 1b: Increase of pyrolysis temperatures during biochar production will decrease the rate of production and subsequently, increase the proportion of C in biochar and thermal stability.

Hypothesis 1c: The type of feedstock will affect the production rate and yields, thermal stability, elemental composition of biochars and overall cation exchange qualities in soil

Objective 2: To assess the effects of biochar application with different feedstock on changes in soil chemical and physical properties.

Hypothesis 2a: Addition of biochars to soil at a common rate of application will improve soil moisture retention due to a significant increase in soil porosity.

Hypothesis 2b: Biochar application will increase retention of soil chemical substrates by adsorbing onto inner and outer surfaces.

Hypothesis 2c: Addition of biochar to soils will increase the soil cation exchange capacity.

Objective 3: To determine the effects of biochar added to selected soils on soil greenhouse gas flux (i.e., CO_2, N_2O and CH_4) with respect to time, temperature, pH and moisture as compared to unamended soils.

Hypothesis 3a: Biochar derived from selected feedstock will decrease soil CO_2, N_2O and CH_4 emissions.

Hypothesis 3b: Addition of biochar in soil will increase the ability of soil to adsorb and retain greenhouse gas substrates (CO_2, N_2O and CH_4) as compared to unamended soils.

REFERENCES

Anderson CR, Condron LM, Clough TJ, Fiers M, Stewart A, et al. (2011) Biochar induced soil microbial community change: Implications for biogeochemical cycling of carbon, nitrogen and phosphorus. Pedobiologia 54: 309– 320.

Asai H, Samson BK, Stephan HM, Songyikhangsuthor K, Homma K, et al. (2009) Biochar amendment techniques for upland rice production in Northern Laos 1. Soil physical properties, leaf SPAD and grain yield. Field Crops Research 111: 81–84.

Biederman LA, Harpole WS (2013) Biochar and its effects on plant productivity and nutrient cycling: a meta-analysis. GCB Bioenergy 5: 202–214.

Blackwell P, Krull E, Butler G, Herbert A, Solaiman Z (2010) Effect of banded biochar on dryland wheat production and fertiliser use in southwestern Australia: an agronomic and economic perspective. Soil Research 48: 531–545.

Cheng C-H, Lehmann J, Thies JE, Burton SD, Engelhard MH (2006) Oxidation of black carbon by biotic and abiotic processes. Organic Geochemistry 37: 1477–1488

Glaser B, Balashov E, Haumaier L, Guggenberger G, Zech W (2000) Black carbon in density fractions of anthropogenic soils of the Brazilian Amazon region. Organic Geochemistry 31: 669–678.

Glaser B, Haumaier L, Guggenberger G, Zech W (2001) The 'Terra Preta' phenomenon: a model for sustainable agriculture in the humid tropics. Naturwissenschaften 88: 37–41.

International Biochar Initiative (2013) Apr 2013 Update: Biochar Carbon Offset Protocol Submitted for Validation at American Carbon Registry. International Biochar

Initiative website. Available: http://www.biochar-international.org/ protocol. Accessed 27 Aug 2013.

International Biochar Initiative (2013) How much CO2 can biochar potentially remove from the atmosphere?: International Biochar Initiative website. Available: http://www.biochar-international.org/biochar/faqs#q10. Accessed 16 Mar 2017.

International Biochar Initiative (2013) International Policy. International Biochar Initiative website. Available: http://www.biochar-international.org/ policy/international. Accessed 16 Mar 2017.

International Biochar Initiative (2013) What Is Biochar? International Biochar Initiative website. Available: http://www.biochar-international.org/biochar. Accessed 27 Aug 2013. 22.

Jeffery S, Verheijen FGA, van der Velde M, Bastos AC (2011) A quantitative review of the effects of biochar application to soils on crop productivity using meta-analysis. Agriculture Ecosystems & Environment 144: 175–187.

Kammann CI, Linsel S, Gossling JW, Koyro HW (2011) Influence of biochar on drought tolerance of Chenopodium quinoa Willd and on soil-plant relations. Plant and Soil 345: 195–210.

Karami N, Clemente R, Moreno-Jimenez E, Lepp NW, Beesley L (2011) Efficiency of green waste compost and biochar soil amendments for reducing lead and copper mobility and uptake to ryegrass. Journal of Hazardous Materials 191: 41–48.

Karhu K, Mattila T, Bergstrom I, Regina K (2011) Biochar addition to agricultural soil increased CH4 uptake and water holding capacity - Results from a short-term pilot field study. Agriculture Ecosystems & Environment 140: 309– 313.

Kookana RS, Sarmah AK, Van Zwieten L, Krull E, Singh B (2011) Biochar application to soil: Agronomic and environmental benefits and unintended consequences. In: Sparks DL, editor. Advances in Agronomy, Vol 112. pp. 103– 143.

Laird DA, Brown RC, Amonette JE, Lehmann J (2009) Review of the pyrolysis platform for coproducing bio-oil and biochar. Biofuels Bioproducts & Biorefining-Biofpr 3: 547–562.

Lal R (2004) Soil carbon sequestration impacts on global climate change and food security. Science 304: 1623–1627.

Lal R, Follett RF, Stewart BA, Kimble JM (2007) Soil carbon sequestration to mitigate climate change and advance food security. Soil Science 172: 943– 956 910.1097/ss.1090b1013e31815cc31498.

Larson RW (2009) Using biochar for cost-effective CO_2 sequestration in soils. Springer. pp. 2462–2467

Magdoff F, Van Es H (2009) Building soils for better crops: sustainable soil management 3rd edn. Sustainable Agriculture Network handbook series 10. Sustainable Agriculture Publications, Waldorf, MD.

Matovic D (2011) Biochar as a viable carbon sequestration option: Global and Canadian perspective. Energy 36: 2011–2016.

Moher D, Liberati A, Tetzlaff J, Altman DG, Group TP (2009) Preferred Reporting Items for Systematic Reviews and Meta-Analyses: The PRISMA Statement. PLoS Med 6: e1000097.

Paustian K, Six J, Elliott ET, Hunt HW (2000) Management options for reducing CO2 emissions from agricultural soils. Biogeochemistry 48: 147– 163.

Powlson DS, Gregory PJ, Whalley WR, Quinton JN, Hopkins DW, et al. (2011) Soil management in relation to sustainable agriculture and ecosystem services. Food Policy 36: S72–S87.

Roberts KG, Gloy BA, Joseph S, Scott NR, Lehmann J (2010) Life cycle assessment of biochar systems: estimating the energetic, economic, and climate change potential. Environmental Science & Technology 44: 827– 833.

Smith P, Fang C, Dawson JJC, Moncrieff JB (2008) Impact of Global Warming on Soil Organic Carbon. In: Donald LS, editor. Advances in Agronomy: Academic Press. pp. 1–43.

Sohi SP, Krull E, Lopez-Capel E, Bol R (2010) A review of biochar and its use and function in soil. In: Sparks DL, editor. Advances in Agronomy, Vol 105. pp. 47–82.

Spokas KA (2010) Review of the stability of biochar in soils: predictability of O: C molar ratios. Carbon Management 1: 289–303.

CHAPTER 2

CHARACTERIZATION OF AGROFORESTRY FEEDSTOCKS AND THEIR BIOCHARS AS A FUNCTION OF TEMPERATURE USING SOLID-STATE ^{13}C NMR AND FTIR-DRIFTS ANALYSIS

ABSTRACT

The temperature at which biochar (biocharcoal) is produced is a major factor that determines its chemical and structural characteristics. The objectives of this research were to assess the effects of feedstock source among potential agroforestry materials and pyrolysis temperature on changes in biologically-labile and stable carbon and nitrogen forms in the original and pyrolyzed materials, and to compare several methods of chemical characterization and their utility in assessing changes in carbon and nitrogen forms. Three main analytical techniques (advanced solid-state ^{13}C NMR techniques, FTIR-DRIFTS analysis and total carbon and nitrogen analysis) were used to characterize biochar produced at 300 or 500ºC from agroforestry feedstock (i.e., walnut (*Juglans regia*) hulls, switchgrass (*Panicum virgatum*) and cottonwood (*Populus deltoids*) feedstock). Results indicated that at 300°C, biochar was primarily composed of residues of biopolymers, such as lignin, cellulose and hemicellulose, while carbohydrates and most of the ligno-cellulosic features were lost when the temperature was increased to 500°C. These results confirmed other researchers' observations that sp^3-hybridized carbon was lost at 500°C and the biochars became enriched with non-protonated aromatic bridgehead carbons. Decreased protonated aromatic carbons and aromatic C-O functional groups and increased nonprotonated aromatic functional groups were observed with increased pyrolysis temperature. Higher pyrolysis temperatures resulted in biochars that predominantly consisted of aromatic functional groups, and promoted loss of lignin, cellulose and labile biopolymers and carbohydrates from the original feedstock.

INTRODUCTION

Biochar (biocharcoal) is a carbonaceous material comprised of a continuum of black carbon materials (e.g., soot, charcoal, and char) resulting from incomplete low oxygen burning (pyrolysis) of feedstock at relatively high temperatures (Brewer et al., 2009; Mao et al., 2010). Biochars, when employed as a soil amendment, are effective agents as a carbon sink and to sequestering greenhouse gases (GHG), such as CO_2, CH_4 and N_2O (Lehmann et al., 2008). Biochars have been found to be more stable in soils than C in the original feedstock when it is applied to soil. The C compounds in moderate and high temperature biochars are stabilized in soil against microbial decomposition and, therefore, may persist in soils for hundreds of years (Anderson et al., 2011). For millennia, indigenous communities, for instance, in the Terra Preta region of the Amazon rainforest, have employed the charring of feedstock technique as a means to both utilize a source of energy, but also as a way to improve soil fertility (Glaser et al., 2001, 2002).

Use of biochar as a soil amendment has been extensively researched and has been observed to increase carbon sequestration (Glaser et al., 2001, 2002; Lehmann et al., 2006, 2008; Yamato et al., 2006; Chan et al; 2008). Other benefits of biochar amendments include reduced leaching of N into ground water, reduced soil nitrous oxide emissions, improved soil fertility due to increased cation-exchange capacity and well-moderated soil acidity, greater soil water retention capacity, and a larger surface area that promotes higher soil microbial activity (Lal et al., 2004; Lal et al., 2007; Larson et al., 2009; De Gryze et al., 2010; Matovic et al., 2011). Due to these beneficial effects of biochars and the inexpensive process of preparation of this material from a variety of feedstock, biochars have the potential to provide an additional source of revenue for small-scale producers employing agroforestry-farming practices (Yoo and Kang, 2012).

Important parameters affecting biochar production include feedstock type, temperature, and oxygen availability during pyrolysis, duration of pyrolysis, and volatiles evolved during pyrolysis (McBeath et al., 2012). The type of feedstock is a key factor governing the physiochemical properties (i.e., pH, volatile compound content, ash content, bulk density, pore volume, and specific surface area) of the resulting biochar. Pyrolysis temperature is the most significant process parameter that determines the biochar yield in its production through pyrolysis, physical and chemical qualities, such as particle size, water-holding capacity and ash content (Kuwagaki et al., 1990). Differences in pyrolysis conditions and times and absence of additives, such as NaOH, during pyrolysis have been cited as the main factors affecting the disappearance of labile chemical functional groups at the molecular level in biochar (David et al., 2009; McBeath et al., 2011).

Solid-state ^{13}C NMR spectroscopy, which has the advantage to nondestructively detect structural information and changes at the molecular level, is an analytical technique that can be used to characterize biochar (Brewer et al., 2009). The degree of aromatic ring condensation is an important feature for biochar structure, where the observed fused ring size expands tending towards graphite structure with thermal alteration (McBeath et al., 2011). Various methodologies such as the ^{13}C cross-polarization(CP) magic angle spinning (CP/MAS), as well as an approach where wet chemical techniques are employed have previously been explored (David et al., 2009). In these studies, CP/MAS was found to be unreliable in the quantification of aromatic carbons due to the high concentration of stabilized free radicals in biochars that significantly decrease the efficiency of the CP (Brewer et al., 2009; David et al., 2009). Attempts have been made at employing a wet chemical approach where biochars are

oxidized using nitric acid and the resultant single ring aromatic molecules with carboxylic groups attached to them (benzene polycarboxylic acids/BPCAs), and later qualitative assessment of the benzene clusters being inferred (Brewer et al (2009); Mao et al (2006, 2010)). While it was a plausible method, it could fail due to the difficulty associated with spectral separation of bridgehead C from other nonprotonated aromatic C. Other methods that have been explored by Smernik and McBeath et al. (2009, 2011) involved the use of ^{13}C-labelled benzene to biochars and thereafter tracking changes in chemical shifts of benzenes sorbed into the biochars. Ultimately, Brewer et al (2009) proposed an NMR-based methodology employing long-range ^{1}H-^{13}C dipolar dephasing and spectral analysis.

The objective of this research was to characterize the structures of three feedstock types (i.e., walnut hulls, switchgrass and cottonwood) derived from temperate agroforestry practices and their respective biochars prepared at thermal variations (300 and 500^{o}C) using advanced solid-state ^{13}C NMR techniques and dipolar dephasing. This characterization also used analyses from corresponding FTIR spectra as well as data from total carbon and nitrogen analyses. By integrating the NMR peaks and relating them to the total C content in each component, the mean concentration of ^{13}C NMR functional groups was determined based on a methodology proposed by Mao et al. (2006). A second objective of the research was to track recalcitrance, based on observing changes in different aromatic C forms (aromatic C-C, aromatic C-H, aromatic C-O, aromatic edge C, and/or bridgehead C). This technique quantifies and tracks disappearance of functional groups characteristic of lignin, cellulose and hemicellulose as a function of temperature (Cao et al. (2012). The information generated from this research may assist in further

assessment of the value of biochar for production by agroforestry practitioners and its potential uses for environmental management.

MATERIALS AND METHODS

Initial Feedstock Conditions and Biochar Preparation

Feedstock samples of switchgrass (*Panicum virgatum*) in its mature stage of growth, walnut (*Juglans regia*) hulls (byproducts of de-hulling of mature walnuts collected from the open field), and cottonwood (*Populus deltoides*) branches in the seed-producing and dissemination stage (~5 years old), were obtained from the University of Missouri Horticulture and Agroforestry Research Center (HARC) in New Franklin, MO (USA) in Fall of 2016. The switchgrass and cottonwood feedstock obtained were air-dried on site. The feedstock samples were later oven-dried at 60-80^{o}C in a forced-air oven for 24 hours and then ground to pass through a 1 mm sieve before being subjected to pyrolysis and subsequent analyses.

A Parr Pressure Reactor (Parr Instrument Company-Moline, Illinois, USA), equipped with a 500 mL stainless steel cylinder, was used to convert feedstock into biochar. Each feedstock type was separately fed and firmly compacted into the stainless-steel cylinder designed to fit into a ceramic fiber furnace that heats up to a temperature of 500^{o}C, raising the reactor pressure up to 34.5 MPa. The reactor cylinder was tightly sealed for pyrolysis and a pressure gauge attached before being inserted into the furnace. Oil and/or non-condensable gases evolved during the slow pyrolysis process were released throughout the pyrolysis process through the stainless-steel fittings and vents. The furnace controller was programmed to drive the internal feedstock chamber temperature to 300^{o}C at a rate of 20^{o}C min^{-1} for one set of samples and 500^{o}C for another set of samples. The samples were kept at the target temperature for ~2 h before cooling to

room temperature. Biochar produced in the pyrolysis was gently crushed and sieved into <2 mm size fractions to minimize presence of residual ash particles using a 2 mm sieve.

The total C and total N in switchgrass, walnut hulls and cottonwood feedstock and their corresponding biochars prepared at 300 and 500 ^{o}C pyrolysis temperatures, were measured using an elemental analyzer on a LECO TruMac C/N analyzer (LECO Corp., St. Joseph, MI.

Parameters for ^{13}C Solid NMR Spectroscopy

A Bruker Avance DRX300 widebore NMR spectrometer equipped with a 7 mm CPMAS probe was employed to perform ^{13}C NMR analyses. About 200 mg of the materials were finely ground using a mortar and pestle into <1 mm size fractions. The fineness of the fractions was visually estimated. Sample was packed into a 7 mm Zirconia rotor with Kel-F cap which was then spun at 5 kHz at room temperature. The operating frequency was 300.13 MHz for proton and 75.48 MHz for carbon, respectively. Cross-polarization with magic angle spinning and total sideband suppression (CPTOSS[1]) was acquired with a 1-ms contact time and 2.03 s repetition delay. A total 2048 scans were collected for each sample (slightly over one hour experiment time). Line broadening of 300 Hz (biochar) and 50 Hz (feedstock) was applied to the FID before Fourier Transformation. The ^{13}C chemical shift was externally referenced to the carbonyl carbon signal of glycine at 176.03 PPM. CPTOSS with dipolar dephasing (CPTOSSDD[2]) was done under the identical condition as that of CPTOSS except a 40-µs (char) and 25-µs (feedstock) were inserted in the TOSS sections of the CPTOSS pulse sequence. Proton decoupling was turned off during the period that the ^{13}C Solid NMR dipolar dephasing was performed (Lehmann, 2009).

FTIR-DRIFTS Spectroscopy

The feedstock samples and their corresponding 300 and 500 ^{o}C biochars were oven-dried for 24 hours at 60^{o}C and ground using a mortar and pestle, sieved through a 1 mm sieve, and kept in a sealed desiccator for 24 hours to keep the samples dry. An FTIR Sample Technique that employs the Diffuse Reflectance (DRIFTS) was performed using a Digilab FTS (Varian Inc., Agilent Technologies) with a DTGS detector and a KBr beam splitter was used to conduct analysis of the samples. Potassium bromide was used as background and was subtracted from each recorded spectrum. Four hundred scans were done in diffuse reflectance from 4000 to 400 cm^{-1} on samples diluted to 10% sample in KBr.

Spectral Analysis with NMR and FTIR

Use of ^{13}C Solid State NMR to determine feedstock and their respective biochar chemical functional groups provides enhanced signal-to-noise ratio (Cao et al., 2012), reducing the amount of time spent in experimentation. ^{13}C NMR spectral outlines were obtained using dipolar dephasing technique, which clarifies signals from nonprotonated carbons and mobile carbon groups (Cao et al., 2012). Dipolar dephasing allows for better quantitative chemical composition of feedstock types and their representative biochars under analysis. It allows for a sharper and prominent peaks of –COOR functional groups, aromatic C–O, delocalized $(CH_2)_n$ groups, nonprotonated C–C functional groups, methoxy carbons, and peaks of methyl carbons. Observations of peaks belonging to –OCH_3 carbons, aromatic C–C carbons and aromatic C–O carbons is enhanced with additional spectral clarification of weak signals representative of –OCH_3 and –CCH_3 carbons which exist in lower concentrations. Enrichment and subsequent domination of peaks related to nonprotonated aromatic carbons at ~150^{o}C with increase in pyrolysis temperature, concurrently accompanied by gradual depletion and disappearance of –

OCH_3 functional groups, aromatic C–O groups and methyl carbons is further observed and confirmed. Dipolar dephasing is chosen for this experiment because of its proven reliability in quantification of various chemical compositions of all feedstock types and their respective biochars, which in this case were prepared at 300 and 500°C pyrolysis temperatures.

FTIR spectra obtained show signals of all functional groups containing the characteristics of untreated and pyrolyzed feedstock samples. Signals from the following functional groups were observed: (a) broad phenolic –OH and –NH functional groups at 3420cm^{-1}; (b) C=O at 1740 cm^{-1}; (c) Alkyl C–H stretch (2900 cm^{-1}). Presence of these functional groups are a confirmation of the presence of hemicellulose (CH_3COO), lignin ($ArOCH_3$), $–OCH_2$ of cellulose and –OCH functional groups characteristic of cellulose, hemicellulose and lignin (Chia et al., 2012). This result corroborates analyses of functional groups using NMR spectroscopy.

RESULTS AND DISCUSSION

Solid State NMR Spectroscopy

Spectra are presented from ^{13}C Solid State Nuclear Magnetic Resonance (NMR) analysis of walnut hulls, switchgrass and cottonwood feedstock and their respective corresponding biochars prepared at 300 and 500°C. The ^{13}C NMR spectra (Figure 2.1) shows signals for the untreated feedstock types and are typical of spectra obtained from unaltered feedstock (Solum et al., 1995; Czimczik et al., 2002; Mao et al., 2006; Ascough et al., 2008). Functional groups of interest that were observed in the ^{13}C NMR spectra (Freitas et al., 1999; Mao et al., 2006; Cao et al., 2012) were: (a) weak signals corresponding to $COOR/CH_3COO$ functional groups at 173 ppm; (b) oxygenated aromatic carbons (148 ppm); (c) non-oxygenated aromatic carbons between 110 - 140

ppm; (d) a sharp peak for di-O-alkyl carbons at 103 ppm; (e) –OCH groups resonating for C_4 carbons of cellulose and Cβ carbons of cellulose and C_3 and C_5 carbons of cellulose and hemicellulose at 72 ppm; (g) O-Alkyl carbon groups representative of $–OCH_2$ carbons and C6 carbons of cellulose at 62 ppm; (h) methoxyl carbons characteristic of $ArOCH_3$ of lignin found in the 45 – 62 ppm range; (i) methylene carbons (30 ppm); (j) alkyl carbons and methyl functional groups signifying peaks representative of CH_3COO of hemicellulose. These peaks are cumulatively representative of biopolymers including cellulose and/or hemicellulose sharing chemical shifts at 62, 72, 82 and 103 ppm, and lignin characterized by peaks appearing at 57, 128 and 148 ppm in untreated feedstock (Tables 2.1, and 2.2).

^{13}C NMR spectra in biochars prepared at 300^oC represented in the spectra (Figure 2.2, 2.3 and 2.4) show that the significant spectral transformations denote similar major structural and chemical changes in all the three different feedstock types with an increase in pyrolysis temperature. These results corroborate observations by Cao et al. (2012) that an increase in pyrolysis temperature will result in subsequent development of broader alkyl carbon signals as well as an appearance of a small signal downfield beyond 200ppm, a chemical shift characteristic of ketone and/or aldehyde carbons. Additionally, these results show enrichment of aromatic carbons and methylene ($-OCH_3$), and a significant shrinking of signals of O-alkyl and di-O-alkyl carbon functional groups.

Major spectral transformations were observed with a further increase in pyrolysis temperature up to 500^oC, where complete disappearance of O-alkyl and di-O-alkyl carbons takes place (Freitas et al., 1999). On the other hand, an increase in in the intensity and dominance of aromatic resonance at ~148ppm, indicated the disappearance of cellulosic features of feedstock and a concurrent alteration of functional groups

representative of lignin and cellulose (Mao et al., 2006). Intensities of spectra characterizing oxygenated functional groups (~152ppm) decrease and broader and well-defined aromatic bands emanate and increase in amplitude. Similar findings have been reported by other groups (Solum et al., 1995; Freitas et al., 1999; Cao et al., 2012) in their studies of biochar from feedstock including white oak, peat and rice hulls prepared at above 500°C pyrolysis temperatures. These studies found that a larger number of delocalized π electrons surrounding the ^{13}C nuclei due to an increase in the amount of aromatic carbons with an increase in pyrolysis temperature was responsible for the broadening of the aromatic carbon spectrum at ~148ppm chemical shift.

Previous research by different groups using NMR spectroscopic method to study biochars from various feedstock types have corroborated the results observed in this research. Several studies reported the enrichment of aromatic carbons and the depletion of all other labile nonaromatic functional groups with the increase in pyrolysis temperature (Pastorova et al., 1994; Freitas et al., 1999; Czimczik et al., 2002; David et al., 2009; McBeath et al., 2011; Cao et al., 2012). Baldock et al. (2002) and David et al. (2009) also reported a significant reduction in the cellulose NMR signature in contrast with Cao et al. (2012), whose group reported an insignificant depletion of cellulose at 300°C.

Our research confirmed 300-500°C as being within the temperature range for pyrolysis at which different feedstock materials experience significant loss of their ligno-cellulosic features, (Freitas et al., 1999). McBeath et al. (2011) reported a rapid increase in the aromaticity of wood biochars through the low temperature range of 250-450°C, exceeding 89% at 400°C pyrolysis temperatures and 99-100% aromaticity at temperatures above 400°C.

The most significant finding of this research that was observed was that after pyrolysis, there were very slight and therefore almost undistinguishable difference among the biochars from the various feedstocks. Slightly lower concentrations of ~85% aromatic carbon concentrations at 500^{o}C between 173.8-96.0 ppm chemical shifts on the NMR were also observed as compared to the results of McBeath et al. (2009). Cao et al. (2012), whose results more closely match those of this research. They attribute the slight discrepancy to differences in pyrolysis conditions (e.g., heating rate, and treatment time) and their severe spinning sidebands which were a probable source of uncertainty in their estimation of aromaticity.

FTIR-DRIFTS Spectroscopy

FTIR analysis and determination of total C/N concentrations as a function of temperature corroborated aromatic carbon concentrations and the presence of functional groups in feedstock observed with NMR spectroscopy. These findings are shown in spectra obtained from the FTIR-DRIFTS analysis of cottonwood, walnut hulls and switchgrass feedstock and their corresponding biochars prepared at 300 and 500^{o}C.

The intensity of the –NH and –OH functional group peaks rapidly decrease when walnut hulls, switchgrass and cottonwood feedstock were subjected to pyrolysis at 300^{o}C, suggesting that -OH and -NH groups are unstable at elevated temperatures (Husain et al., 2010). Peaks subsequently appear for aromatic carbonyl/carboxyl C=O groups at 1705 cm^{-1}, which were absent for the feedstock.

Methyl groups (CH_3) disappear alongside –HN and –OH functional groups during pyrolysis. The broad band that corresponds to vibrations at 1544cm^{-1} is observed only in the feedstock samples, a phenomenon also confirmed by Hossain et al. (2011).

At 500°C, removal of aliphatic C-H at 2920 cm^{-1}, phenolic C-O band at 1255 cm^{-1}, and polysaccharide C-O at 1130 cm^{-1} were observed. Bands at 3050 cm^{-1} and 1600 cm^{-1} are indicative of the presence of aromatic C-H and O-H created between 300-500°C. The main difference between the FTIR spectra obtained from this experiment and biochars analyzed in other research studies is this research had additional use of advanced ^{13}C NMR with CP-TOSS alongside C/N analyses to track structural and chemical transitions and transformations in agroforestry feedstock.

Total Carbon/Nitrogen Measurements

A gradual enrichment of carbon content was observed and an observed increase in nitrogen content was revealed with increase in pyrolysis temperature, except for cottonwood. Biochars prepared at 500°C have total C concentrations of >75% while those prepared at 300°C have a carbon content of between 60 to 70%. Therefore, for most of the materials, the biochar C/N ratios increased with increase in pyrolysis temperature, also confirming the finding of Cao et al. (2012) of a significant positive correlation (R^2=0.99) in carbon content with respect to temperature. This is closely associated with chemical reactions that occur during pyrolysis including dehydration and condensation.

A decrease in total N content with pyrolysis from ~1% in feedstock to ~0.5% for grass, hulls and woody biochars was also confirmed by Cao et al. (2012) in a similar observation, while an increase in ash content with increase in temperature is expected and confirmed by the reduction of chemical functional groups that form the building blocks of plant organic matter.

CONCLUSIONS

All the biochars were chemically similar with respect to ^{13}C NMR and FTIR-DRIFTS spectroscopic analyses. Pyrolysis temperature is therefore a significant factor

that drives the chemical and structural transformations that take place in feedstock. It therefore does not matter which material is used for pyrolysis as you a similar chemical composition.

Switchgrass, cottonwood and walnut hulls feedstock and their biochars produced at 300 and 500°C were analyzed and the changes in structural characteristics determined as a function of pyrolysis temperature using advanced ^{13}C NMR spectroscopy with the implementation of the CP-TOSS technique to further improve the spectra. Results from the NMR analysis corroborated with total C and N determination as well as FTIR-DRIFTS spectroscopic analysis indicated enrichment of aromatic characteristics of biochars with an increase in pyrolysis temperature. A decrease in protonated aromatic carbons and aromatic C-O functional groups was observed between 300-500°C, whereas nonprotonated aromatic functional groups increased with an increase in pyrolysis temperature.

Subjecting feedstock to pyrolysis at 300°C results in biochars that exhibited a relative decrease in ligno-cellulosic characteristics. At 500°C, biochars acquired molecular traits that predominantly consisted of aromatic functional groups, while there was concurrent total loss of lignin, cellulose and other labile biopolymers and carbohydrates. Similarities in structure between the biochars of cottonwood, switchgrass and walnut hulls confirm that the various organic functional groups in feedstock undergo similar reactions to form similar deprotonated aromatic functional groups appearing at well-defined chemical shifts and possessing strong and prominent peaks in both the ^{13}C NMR and FTIR spectra.

During biochar production, decrease in concentrations of total N with increase in pyrolysis temperature takes place. On the other hand, concentrations of total C increased from ~50% in feedstock to ~65% in 300^{o}C biochars, and ~85% in 500^{o}C biochars.

Our results suggest that conversion of agroforestry feedstock ranging from grasses to woody material and even hulls and husks to biochar results in biochars with similar chemical compositions, therefore, enabling farmers to be able to pyrolyze any agroforestry feedstock to yield a similar product across feedstock types. This process would not only improve management of agricultural organic waste, but also increase the utilization of resultant biochars as valuable soil amendment products. Benefits of these products may include slow-release of plant nutrients, improved C sequestration, and effects on soil processes, such as soil greenhouse gas emissions.

REFERENCES

Ascough, P. L.; Bird, M. I.; Wormald, P.; Snape, C. E.; Apperley, D. Influence of production variables and starting material on charcoal stable isotopic and molecular characteristics. Geochim. Cosmochim. Act a2008, 72 (24), 6090−6102.

Baldock, J. A.; Smernik, R. J. Chemical composition and bioavailability of thermally, altered Pinus resinosa (Red Pine) wood. Org. Geochem. 2002, 33 (9), 1093−1109.

Bardet, M.; Hediger, S.; Gerbaud, G.; Gambarelli, S.; Jacquot, J. F.; Foray, M. F.; Gadelle, A. Investigation with C-13 NMR, EPR, and magnetic susceptibility measurements of char residues obtained by pyrolysis of feedstock. Fuel 2007, 86 (12−13), 1966−1976.

Brewer, C. E.; Schmidt-Rohr, K.; Satrio, J. A.; Brown, R. C. Characterization of biochar from fast pyrolysis and gasification systems. Environ. Prog. Sustainable Energy 2009, 28 (3), 386−396.

Brodowski, S.; Rodionov, A.; Haumaier, L.; Glaser, B.; Amelung, W. Revised black carbon assessment using benzene polycarboxylic acids. Org. Geochem. 2005, 36 (9), 299−1310.

Chia C.H., Gong B., Joseph S.D., Marjo C.E., Munroe P., Rich A.M. Imaging of mineral-enriched biochar by FTIR, Raman and SEM-EDX Vib Spectrosc, 62 (2012), pp. 248-257

Czimczik, C. I.; Preston, C. M.; Schmidt, M. W. I.; Werner, R. A.; Schulze, E. D. Effects of charring on mass, organic carbon, and stable carbon isotope composition of wood. Org. Geochem. 2002, 33 (11), 1207−1223.

David, K.; Pu, Y.; Foston, M.; Muzzy, J.; Ragauskas, A. Crosspolarization/magic angle spinning (CP/MAS) 13C nuclear magnetic resonance (NMR) analysis of chars from alkaline-treated pyrolyzed softwood. Energy Fuels 2009, 23 (1), 498−501.

Demirbas, A. Feedstock to charcoal, liquid, and gaseous products via carbonization process. Energy Sources 2001, 23 (6), 579−587.

Demirbas, A. Relationships between carbonization temperature and pyrolysis products from feedstock. Energy Explor. Exploit. 2004, 22 (6), 411−419.

Dittmar, T. The molecular level determination of black carbon in marine dissolved organic matter. Org. Geochem. 2008, 39 (4), 396−407.

Dixon, W. T. Spinning-sideband-free and spinning-sidebandonly NMR spectra in spinning samples. J. Chem. Phys. 1982, 77 (4), 1800−1809.

Freitas, J. C. C.; Bonagamba, T. J.; Emmerich, F. G. C-13 Highresolution solid-state NMR study of peat carbonization. Energy Fuels 1999, 13 (1), 53−59.

Freitas, J. C. C.; Bonagamba, T. J.; Emmerich, F. G. Investigation of feedstock- and polymer-based carbon materials using C-13 high-resolution solid-state NMR. Carbon 2001, 39 (4), 535−545.

Fuwape, J. A. Effects of carbonization temperature on charcoal from some tropical trees. Bioresour. Technol. 1996, 57 (1), 91−94.

Glaser, B.; Haumaier, L.; Guggenberger, G.; Zech, W. Black carbon in soils: The use of benzenecarboxylic acids as specific markers. Org. Geochem. 1998, 29 (4), 811−819.

Glaser, B.; Haumaier, L.; Guggenberger, G.; Zech, W. The Terra Preta phenomenon: A model for sustainable agriculture in the humid tropics. Naturwissenschaften 2001, 88 (1), 37−41.

Glaser, B.; Lehmann, J.; Zech, W. Ameliorating physical and chemical properties of highly weathered soils in the tropics with charcoal A review. Biol. Fertil. Soils 2002, 35 (4), 219−230.

Gundale, M. J.; DeLuca, T. H. Temperature and source material influence ecological attributes of Ponderosa pine and Douglas-fir charcoal. For. Ecol. Manage. 2006, 231 (1−3), 86−93.

Hammes, K.; Torn, M. S.; Lapenas, A. G.; Schmidt, M. W. I. Centennial black carbon turnover observed in a Russian steppe soil. Biogeosciences 2008, 5 (5), 1339−1350.

Lehmann, J.; Joseph, S. Biochar for Environmental Management: Science and Technology; Earthscan: London/ Sterling, VA, 2009.

Lim, K. O. Quality of cocoa wood charcoal as a function of carbonisation temperature. Feedstock Bioenergy 1993, 4 (4), 301−302.

Link, S.; Arvelakis, S.; Spliethoff, H.; De Waard, P.; Samoson, A. Investigation of feedstocks and chars obtained from pyrolysis of different feedstocks with solid-state C-13 and Na-23 nuclear magnetic resonance spectroscopy. Energy Fuels 2008, 22 (5), 3523−3530.

Hossain M. K., Strezov V., Chan K. Y., Ziolkowski A., Nelson P. F., Influence of pyrolysis temperature on production and nutrient properties of wastewater sludge biochar, J. Environ. Manage. 2011, 92 (223-228).

Mao, J. D.; Cory, R. M.; McKnight, D. M.; Schmidt-Rohr, K. Characterization of a nitrogen-rich fulvic acid and its precursor algae from solid state NMR. Org. Geochem. 2007, 38 (8), 1277−1292.

Mao, J. D.; Fang, X. W.; Lan, Y. Q.; Schimmelmann, A.; Mastalerz, M.; Xu, L.; Schmidt-Rohr, K. Chemical and nanometer scale structure of kerogen and its change during thermal maturation investigated by advanced solid-state 13C NMR spectroscopy. Geochim. Cosmochim. Acta 2010, 74 (7), 2110−2127.

Mao, J. D.; Holtman, K. M.; Scott, J. T.; Kadla, J. F.; SchmidtRohr, K. Differences between lignin in unprocessed wood, milled wood, mutant wood, and extracted lignin detected by 13C solid-state NMR. J. Agric. Food. Chem. 2006, 54 (26), 9677−9686.

Mao, J. D.; Hu, W. G.; Schmidt-Rohr, K.; Davies, G.; Ghabbour, E. A.; Xing, B. S. Quantitative characterization of humic substances by solid-state carbon-13 nuclear magnetic resonance. Soil Sci. Soc. Am. J. 2000, 64 (3), 873−884.

Mao, J. D.; Schmidt-Rohr, K. Accurate quantification of aromaticity and nonprotonated aromatic carbon fraction in natural organic matter by 13C solid-state nuclear magnetic resonance. Environ. Sci. Technol. 2004, 38 (9), 2680−2684.

Mao, J. D.; Schmidt-Rohr, K. Recoupled long-range C−H dipolar dephasing in solid-state NMR, and its use for spectral selection of fused aromatic rings. J. Magn. Reson. 2003, 162 (1), 217−227.

Mao, J. D.; Schmidt-Rohr, K. Separation of aromatic carbon 13C NMR signals from di-oxygenated alkyl bands by a chemical-shiftanisotropy filter. Solid State Nucl. Magn. Reson. 2004, 26 (1), 36−45.

McBeath, A. V.; Smernik, R. J. Variation in the degree of aromatic condensation of chars. Org. Geochem. 2009, 40 (12), 1161− 1168.

McBeath, A. V.; Smernik, R. J.; Schneider, M. P. W.; Schmidt, M. W. I.; Plant, E. L. Determination of the aromaticity and the degree of aromatic condensation of a thermosequence of wood charcoal using NMR. Org. Geochem. 2011, 42 (10), 1194−1202.

Pastorova, I.; Botto, R. E.; Arisz, P. W.; Boon, J. J. Cellulose char structure: A combined analytical Py-GC-MS, FTIR, and NMR study. Carbohydr. Res. 1994, 262 (1), 27−47.

Preston, C. M.; Schmidt, M. W. I. Black (pyrogenic) carbon: A synthesis of current knowledge and uncertainties with special consideration of boreal regions. Biogeosciences 2006, 3 (4), 397−420.

Sander, M.; Pignatello, J. J. Characterization of charcoal adsorption sites for aromatic compounds: Insights drawn from single-solute and bi-solute competitive experiments. Environ. Sci. Technol. 2005, 39 (6), 1606−1615.

Schneider, M. P. W.; Hilf, M.; Vogt, U. F.; Schmidt, M. W. I. The benzene polycarboxylic acid (BPCA) pattern of wood pyrolyzed between 200 °C and 1000 °C. Org. Geochem. 2010, 41 (10), 1082−1088.

Schneider, M. P. W.; Smittenberg, R. H.; Dittmar, T.; Schmidt, M. W. I. Comparison of gas with liquid chromatography for the determination of benzenepolycarboxylic acids as molecular tracers of black carbon. Org. Geochem. 2011, 42 (3), 275−282.

Sharma, R. K.; Hajaligol, M. R.; Smith, P. A. M.; Wooten, J. B.; Baliga, V. Characterization of char from pyrolysis of chlorogenic acid. Energy Fuels 2000, 14 (5), 1083−1093.

Sharma, R. K.; Wooten, J. B.; Baliga, V. L.; Hajaligol, M. R. Characterization of chars from feedstock-derived materials: Pectin chars. Fuel 2001, 80 (12), 1825−1836.

Sharma, R. K.; Wooten, J. B.; Baliga, V. L.; Lin, X. H.; Chan, W. G.; Hajaligol, M. R. Characterization of chars from pyrolysis of lignin. Fuel 2004, 83 (11−12), 1469−1482.

Sharma, R. K.; Wooten, J. B.; Baliga, V. L.; Martoglio-Smith, P. A.; Hajaligol, M. R. Characterization of char from the pyrolysis of tobacco. J. Agric. Food Chem. 2002, 50 (4), 771−783.

Smernik, R. J.; Kookana, R. S.; Skjemstad, J. O. NMR characterization of C-13-benzene sorbed to natural and prepared charcoals. Environ. Sci. Technol. 2006, 40 (6), 1764−1769.

Solum, M. S.; Pugmire, R. J.; Jagtoyen, M.; Derbyshire, F. Evolution of carbon structure in chemically activated wood. Carbon 1995, 33 (9), 1247−1254.

Uchimiya, M.; Wartelle, L. H.; Klasson, K. T.; Fortier, C. A.; Lima, I. M. Influence of pyrolysis temperature on biochar property and function as a heavy metal sorbent in soil. J. Agric. Food Chem. 2011, 59 (6), 2501−2510.

Cao X., Pignatello J. J., Li Y., Lattao C., Chappell M. A., Chen N., Miller L. F., Mao J., Characterization of Wood Chars Produced at Different Temperatures Using Advanced Solid-State 13C NMR Spectroscopic Techniques, Energy & Fuels. 2012, 26 (9), 5983-5991

Zhu, D. Q.; Kwon, S.; Pignatello, J. J. Adsorption of single-ring organic compounds to wood charcoals prepared under different thermochemical conditions. Environ. Sci. Technol. 2005, 39 (11), 3990−3998.

Table 2.1. ^{13}C NMR functional group percent intensities of signals for the untreated feedstock types, derived from spectra obtained from unaltered feedstock

Chemical Shift	Associated Carbons	CW†	SG†	WH†
		---------- % ----------		
173	COOR/CH_3COO Groups	4	2	5
148	Oxygenated Aromatic Carbons	3	3	3
110-140	Non-oxygenated aromatic carbons	9	8	14
103	Di-O-alkyl carbons	19	20	18
82	OCH groups (C_4 carbons of cellulose/Cβ carbons of lignin)	8	10	8
72	OCH groups (C_2, C_3 & C_5 carbons of Cellulose and Hemicellulose)	35	37	32
62	O-Alkyl carbons (OCH_2 Carbons, C_6 Carbons of cellulose)	11	12	9
45-62	Methoxyl carbons ($ArOCH_3$ of Lignin)	5	3	4
30	Methylene carbons	3	2	3
18	Alkyl Carbons & Methyl (CH_3COO of hemicellulose)	4	3	3

†CW, SG and WH refer to cottonwood, switchgrass and walnut hulls, respectively.

Table 2.2. ^{13}C NMR functional group percent concentrations at varied temperatures (°C)

	Feedstock								
	Cottonwood			Switchgrass			Walnut Hulls		
	0[2]	300	500	0	300	500	0	300	500
Chemical shift	%								
209.7-176.7	0	7	2	2	8	10	3	9	1
173.8-96.0	50	76	92	47	70	72	55	68	85
84.9-51.2	36	4	4	38	7	12	28	7	6
34.8-6.5	14	12	1	14	16	5	15	16	8

[1]Temperature under which pyrolysis was done. [2]Represent non-pyrolyzed feedstock material

Table 2.3. Total carbon and nitrogen concentrations determined during carbon/nitrogen analysis of cottonwood, switchgrass and walnut hulls feedstock and their biochars prepared at varied temperatures (°C).

		Property		
Feed stock material	Temperature	Total C	Total N	C:N ratio
	^0C	%		
Cottonwood	0[1]	50.95	0.88	57.90
	300	72.29	1.58	45.75
	500	75.88	1.87	40.58
Switchgrass	0[1]	49.08	0.53	92.60
	300	65.97	1.93	34.18
	500	72.84	1.04	70.04
Walnut Hulls	0[1]	47.54	1.12	42.45
	300	62.01	1.89	32.81
	500	63.06	1.87	33.72

[1]Represents non-pyrolyzed feedstock material

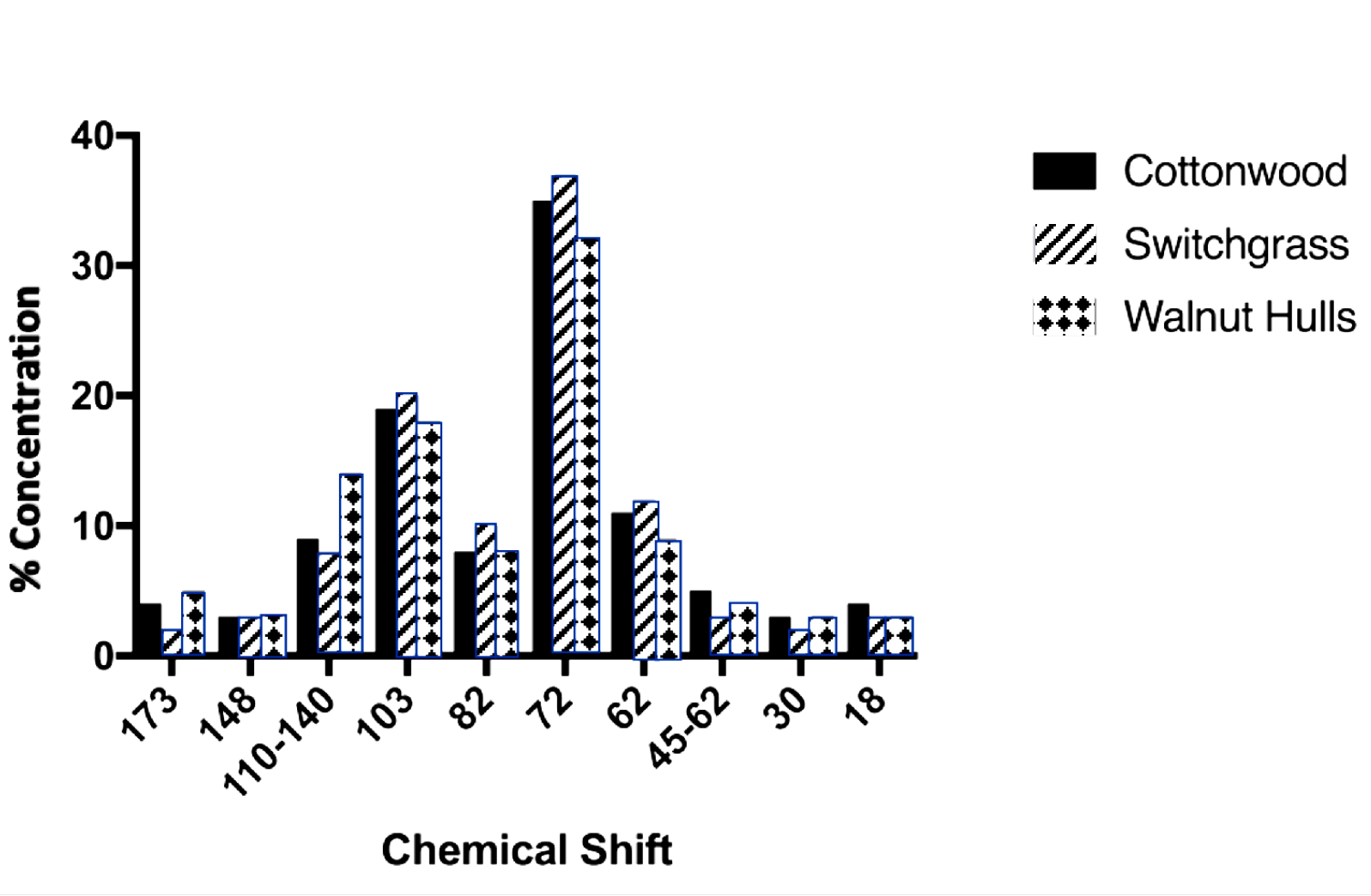

Figure 2.1. Identification of ^{13}C NMR percent concentrations of functional groups for untreated feedstock types between 209 and 0 chemical shifts. Walnut hulls, switchgrass and cottonwood were subjected to ^{13}C NMR spectroscopy to determine the distribution of labile functional groups in order to track the effect of pyrolysis on their concentrations relative to the build-up of recalcitrant aromatic carbon structures.

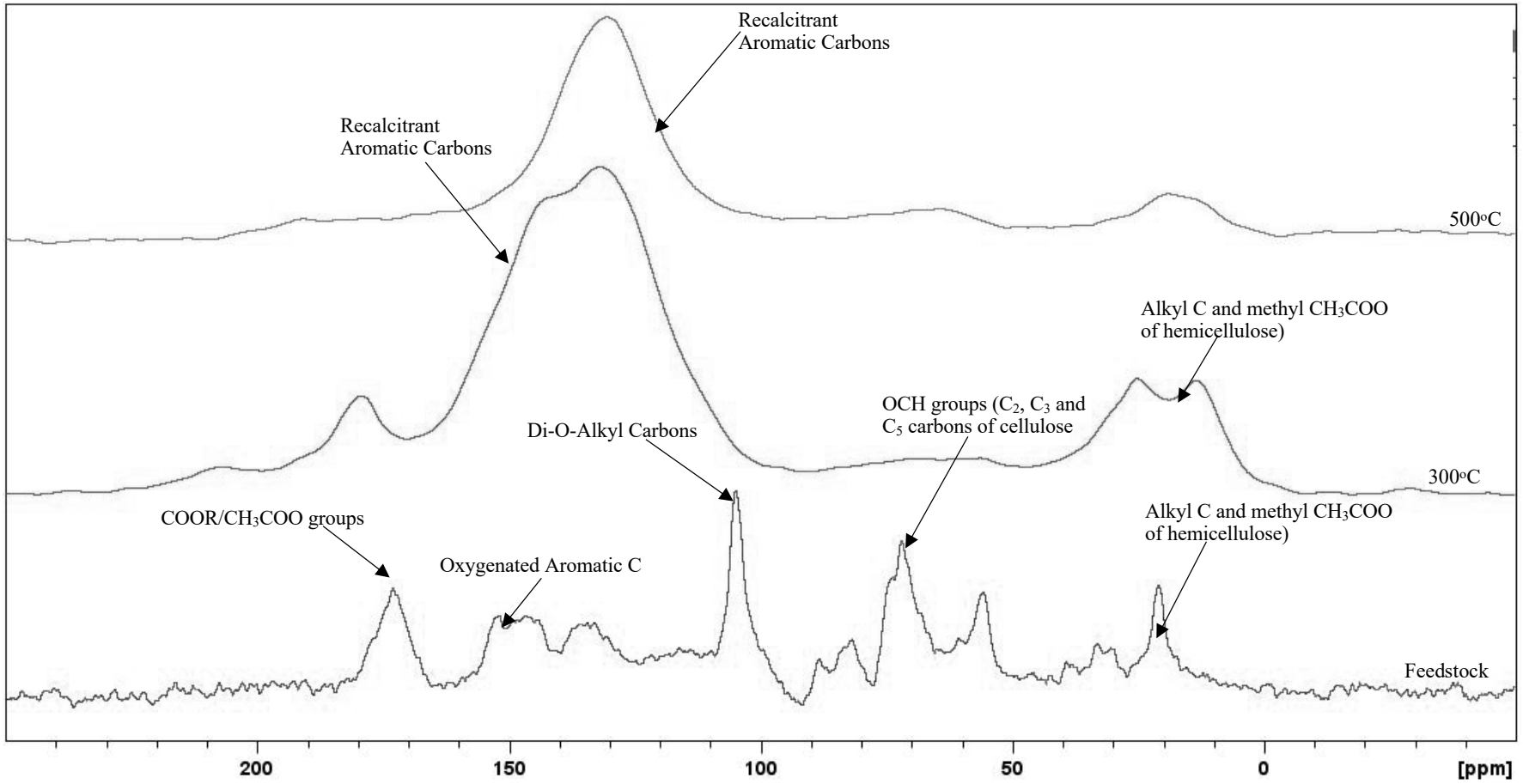

Figure 2.2. Walnut hulls ^{13}C NMR CP-TOSS spectrum of the transformation of functional groups with respect to temperature (Feedstock, 300°C and 500°C from bottom of spectrum to top of spectrum). There is a disappearance of labile COOR/CH_3COO groups, alkyl and methyl CH_3COO of hemicellulose, Di-O-Alkyl Carbons, oxygenated aromatic C, and OCH groups (C_2, C_3 and C_5) carbons of. These functional groups are chemically transformed by pyrolysis into recalcitrant aromatic carbon groups.

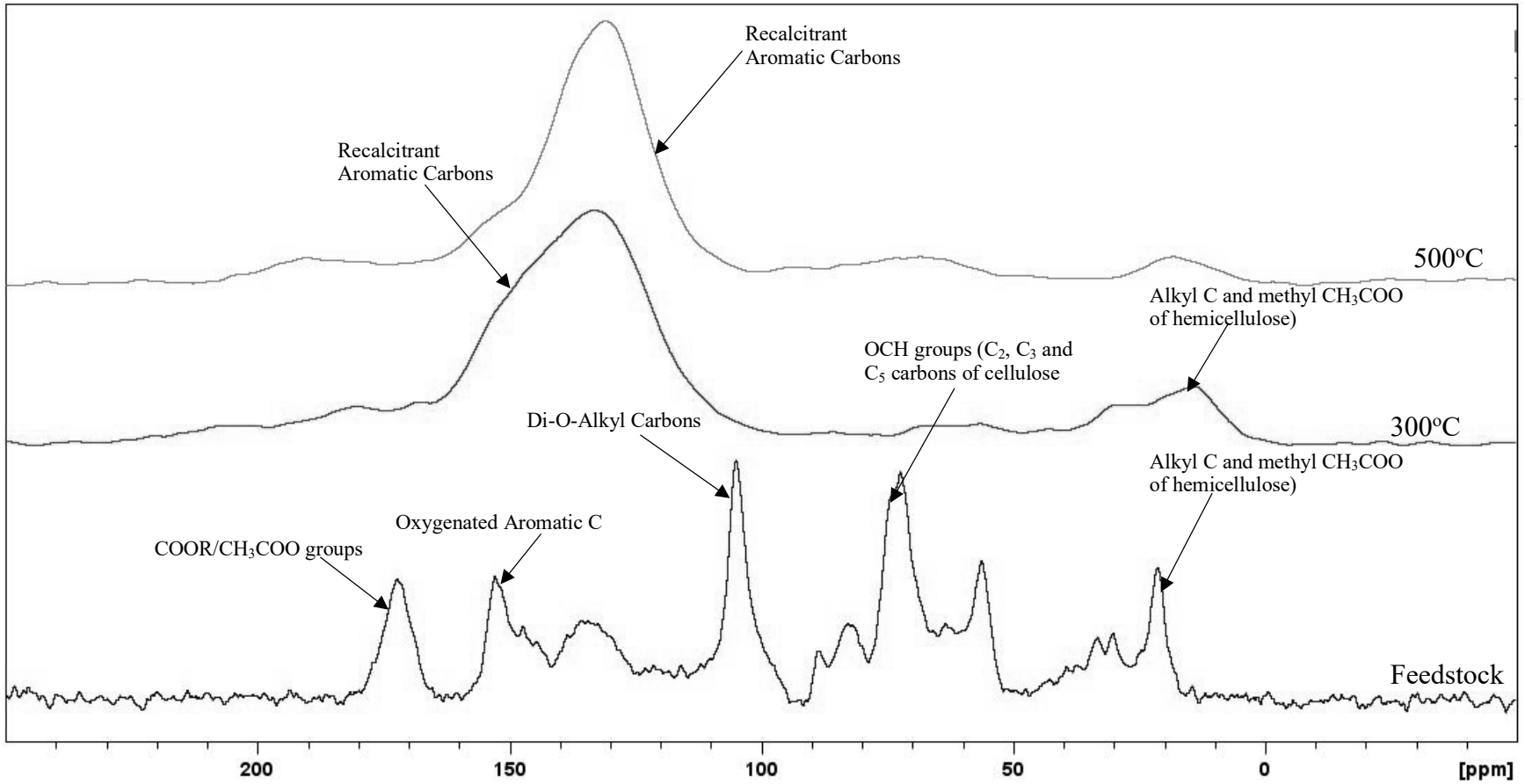

Figure 2.3. Cottonwood ^{13}C NMR CP-TOSS spectrum of the transformation of functional groups with respect to temperature (Feedstock, 300°C and 500°C from bottom of spectrum to top of spectrum). There is a disappearance of labile COOR/CH_3COO groups, alkyl and methyl CH_3COO of hemicellulose, Di-O-Alkyl Carbons, oxygenated aromatic C, and OCH groups (C_2, C_3 and C_5) carbons of. These functional groups are chemically transformed by pyrolysis into recalcitrant aromatic carbon groups.

Figure 2.4. Switchgrass ^{13}C NMR CP-TOSS spectrum of the transformation of functional groups with respect to temperature

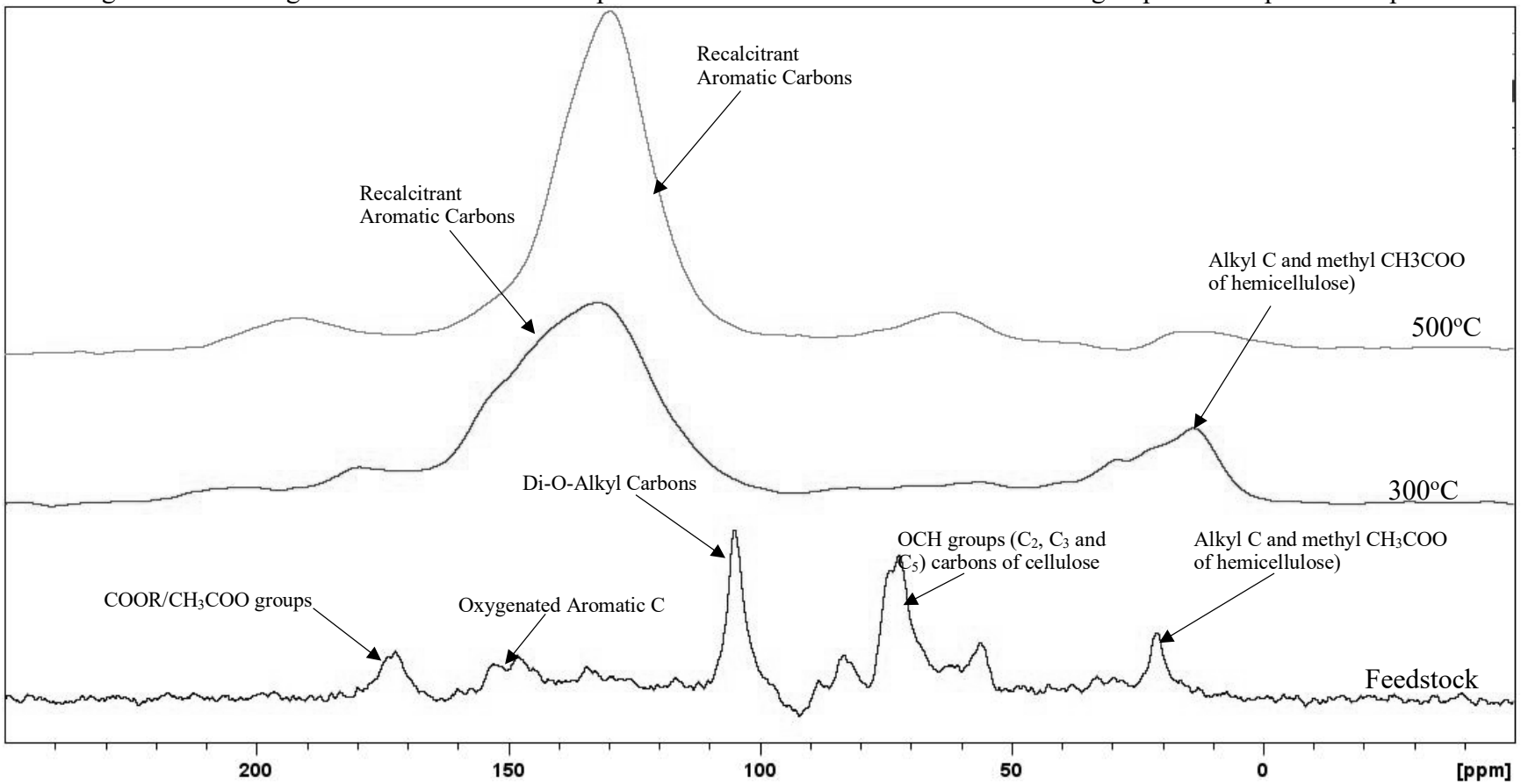

(Feedstock, 300°C and 500°C from bottom of spectrum to top of spectrum). There is a disappearance of labile COOR/CH_3COO groups, alkyl and methyl CH_3COO of hemicellulose, Di-O-Alkyl Carbons, oxygenated aromatic C, and OCH groups (C_2, C_3 and C_5) carbons of. These functional groups are chemically transformed by pyrolysis into recalcitrant aromatic carbon groups.

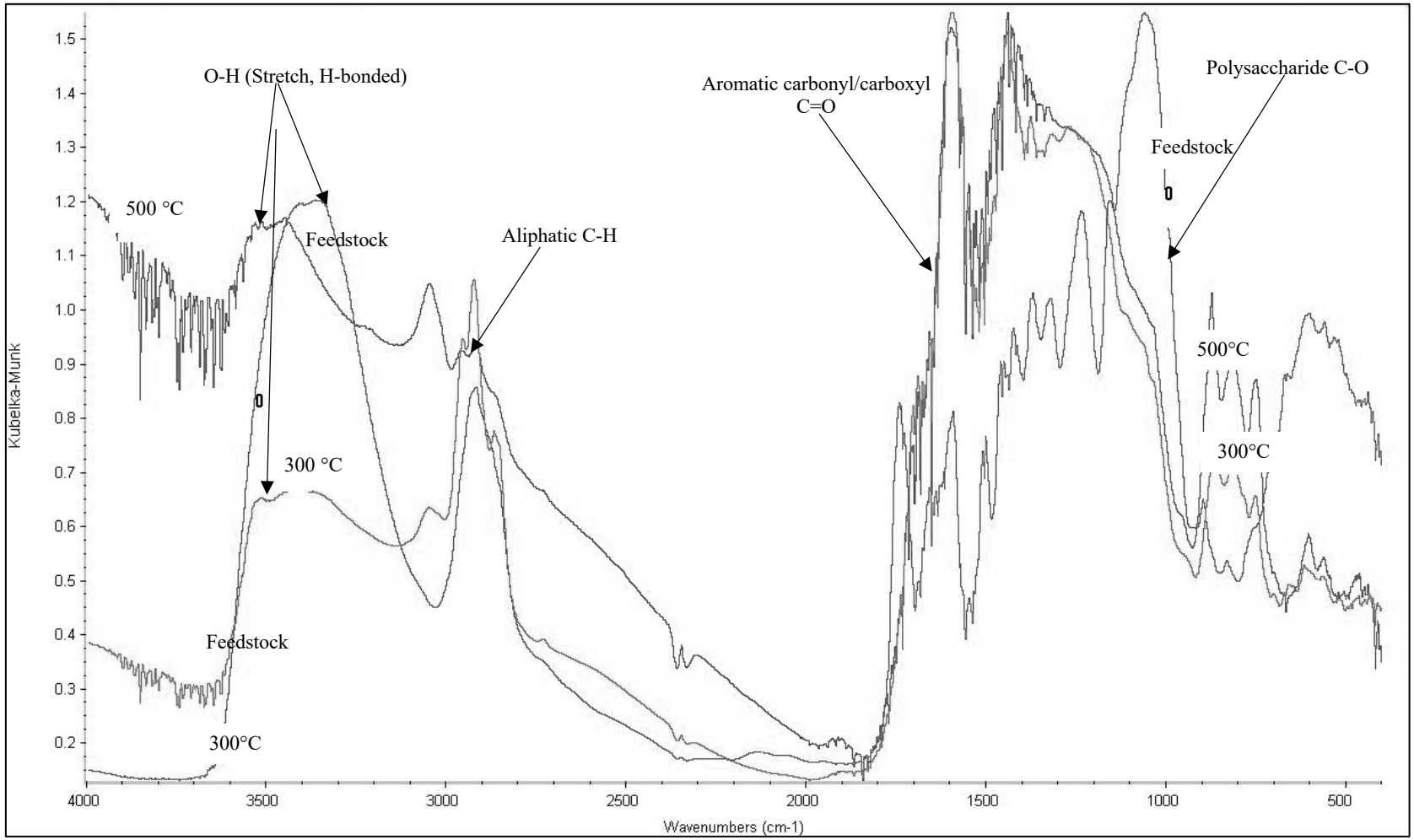

Figure 2.5. Cottonwood FTIR-DRIFTS spectrum of the transformation of functional groups with respect to temperature (Feedstock, 300ºC and 500ºC). The spectrum shows signals from broad phenolic –OH and –NH functional groups at 3420cm^{-1}; C=O at 1740 cm^{-1}; Alkyl C–H stretch (2900 cm^{-1}), as well as Polysaccharide C-O (1100) and aliphatic C-H (2900). These functional groups indicate presence of hemicellulose (CH_3COO), lignin ($ArOCH_3$), $–OCH_2$ of cellulose and –OCH functional groups characteristic of cellulose, hemicellulose and lignin.

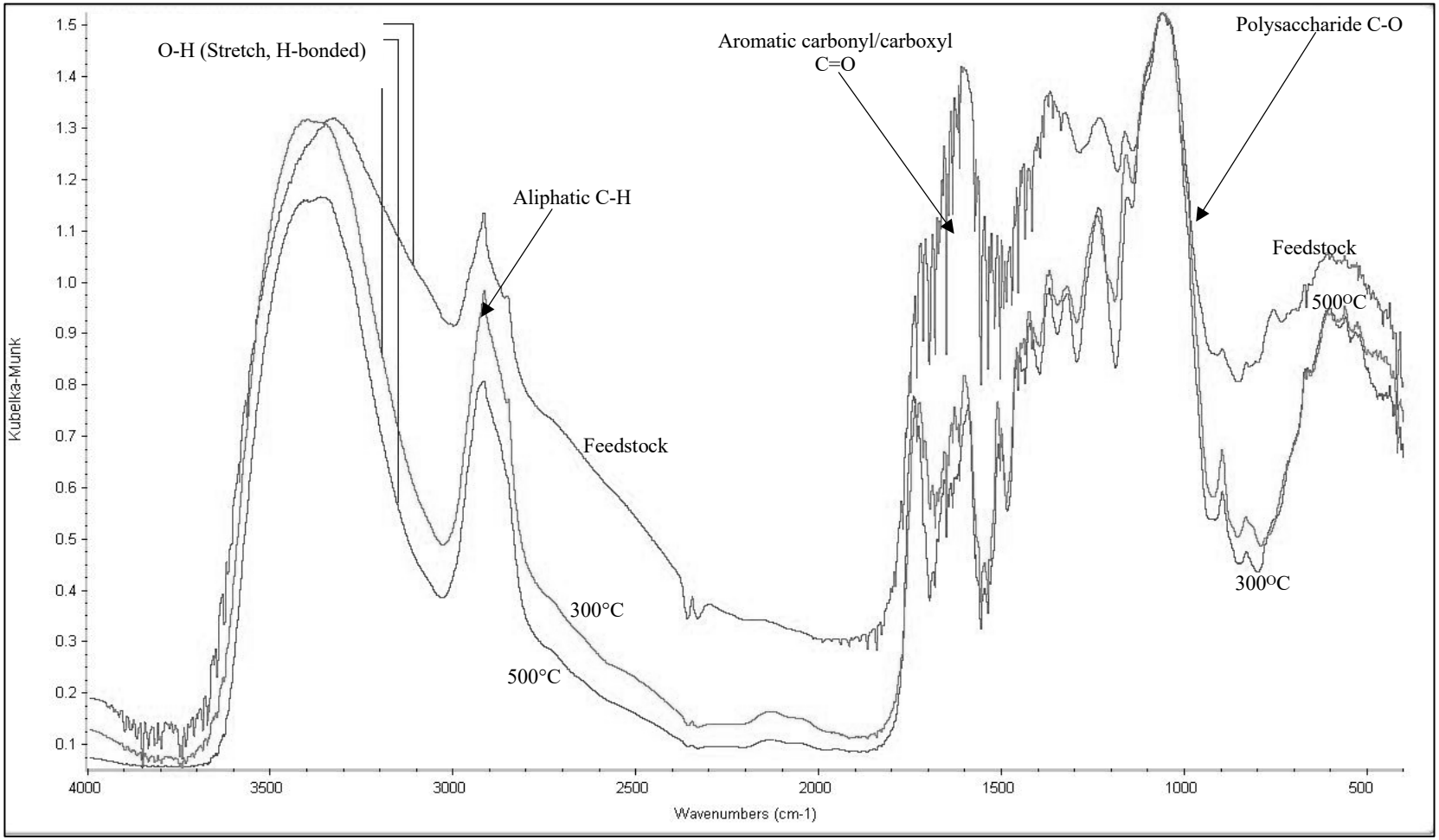

Figure 2.6. Switchgrass FTIR-DRIFTS spectrum of the transformation of functional groups with respect to temperature (Feedstock, 300ºC and 500ºC). The spectrum shows signals from broad phenolic –OH and –NH functional groups at 3420cm^{-1}; C=O at 1740 cm^{-1}; Alkyl C–H stretch (2900 cm^{-1}). These functional groups indicate presence of hemicellulose (CH_3COO), lignin ($ArOCH_3$), $–OCH_2$ of cellulose and –OCH functional groups characteristic of cellulose, hemicellulose and lignin.

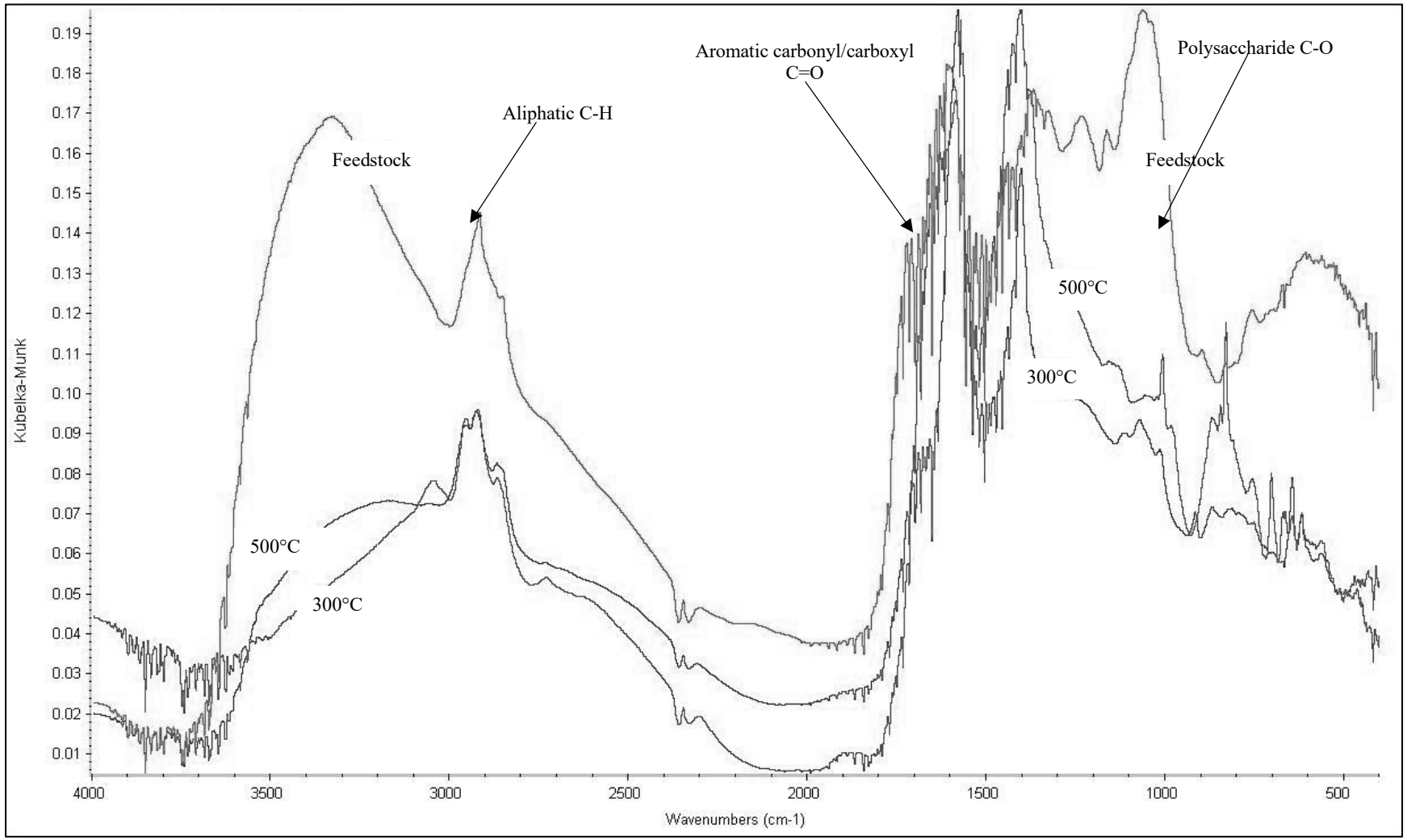

Figure 2.7. Walnut Hulls FTIR-DRIFTS spectrum of the transformation of functional groups with respect to temperature (Feedstock, 300ºC and 500ºC). The spectrum shows signals from broad phenolic –OH and –NH functional groups at 3420cm^{-1}; C=O at 1740 cm^{-1}; Alkyl C–H stretch (2900 cm^{-1}). These functional groups indicate presence of hemicellulose (CH_3COO), lignin ($ArOCH_3$), $–OCH_2$ of cellulose and –OCH functional groups characteristic of cellulose, hemicellulose and lignin.

CHAPTER 3

EFFECT OF BIOCHAR AMENDMENTS FROM AGROFORESTRY FEEDSTOCK ON GREENHOUSE GAS EMISSIONS FROM FLOODPLAIN SOILS

ABSTRACT

Use of biochar, a recalcitrant product of pyrolysis of feedstock, as a soil amendment may be a strategy for greenhouse gas mitigation and soil carbon (C) sequestration in floodplain soils that may be vulnerable to frequent soil waterlogging. Atmospheric nitrous oxide (N_2O), carbon dioxide (CO_2) and methane (CH_4) are potent greenhouse gases that impact climate change. The production of GHG in soil is influenced by several environmental factors including the quantity of live and dead feedstock in the soil, soil temperature and soil water content. Previous research has shown diverging results of the effects of biochar applications on soil greenhouse gas efflux. The objectives of this research were to determine the impact of applications of different biochars obtained from agroforestry practices i.e, walnut (*Juglans regia*) hulls, switchgrass (*Panicum virgatum*) and cottonwood (*Populus deltoids*) on soil N_2O, CO_2 and CH_4 emissions in a floodplain soil at several soil moisture levels. A controlled temperature incubation experiments was conducted to investigate the effect of the biochars applied at an equivalent rate of 50 Mg ha^{-1} on soil CH_4, N_2O and CO_2 emissions with or without addition of N fertilizer in a bulk floodplain soil collected from the Horticulture and Agroforestry Research Center (HARC) located in New Franklin, Missouri, U.S.A. Incubations were done under 60 or 100% WFPS with temperature being kept constant at 35^{o}C. Cumulative soil N_2O emissions were sharply decreased by 30 to 43% in biochar-amended soils with or without addition of N fertilizer. At 60% WFPS, there was a general decrease in cumulative soil CH_4-C emissions ($p<0.001$) with biochar

compared to the incubation controls irrespective of N fertilizer addition. The results show that application of biochar to a floodplain soil significantly decreased soil CO_2 production and N_2O emissions but increased overall cumulative soil CH_4 emissions. The results from this research provide a basis for estimating the potential mitigation of soil greenhouse gas emissions that can be achieved by incorporating biochar into a floodplain soil in Mid-Missouri.

INTRODUCTION

The Mississippi and Missouri River Basin floodplain is an important region for agricultural production and is environmentally sensitive area for multiple reasons including the floodplain's proximity to major water resources, frequent flooding and its importance for wildlife habitat (Rondon et al., 2006; Murage et al., 2007). New land uses, such as biofuel production, in the floodplain may have several environmental consequences due to a possible increase in nutrient use, changes in vegetation and more intensive land preparation (Laird et al., 2008; Liang et al., 2008). The effects of climate change in the region, such as an increased incidence of extreme rainfall events in the spring, may also have environmental consequences including an effect on the total amount and rate of soil greenhouse gas emissions in the floodplain (Schmidt et al., 2000; Khin et al., 2007).

Application of biochar is one potential strategy to sequester soil carbon and subsequently reduce soil greenhouse gas emissions (Glaser et al., 2001, 2002; Lehmann et al., 2006, 2008; Yamato et al., 2006; Chan et al; 2008). Before the multinational resolutions were agreed upon at the 2015 United Nations Climate Change Conference in Paris, France, biochar had been proposed as an option that could be utilized to replenish soil carbon pools, restore soil fertility and sequester greenhouse gas emissions by the

United Nations Convention to Combat Desertification (UNCCD, 2009) to the United Nations Framework Convention on Climate Change.

Biochar is often land-applied at variable rates depending on several factors including the objective of land applying biochar, the properties of the biochar itself, and the cost of biochar and its local availability. Woolf et al (2010), discusses rates of application of biochar to soil for the purpose of climate change mitigation, suggesting a global biochar application rate of 50 Mg ha^{-1} in most agricultural systems. Several studies have reported positive effects of biochar application on crop yields with rates of 5 to 50 Mg of biochar ha^{-1}on a dry weight basis, combined with appropriate nutrient management, (Chan et al., 2007, 2008; Major et al., 2010b). Due to its stability in soil, a single application of biochar can provide beneficial effects over several growing seasons in the field (Steiner et al., 2007; Major et al., 2010b). Biochar, therefore, does not need to be re-applied with each crop, as may occur with other soil amendments, such as synthetic fertilizer. Depending on target application rate, the availability of biochar supply, and the soil management system, biochar amendments can be applied in split applications (Kammann et al., 2012).

Biochar application rates of 10, 25, 50 and 100 Mg ha^{-1} have all been observed to significantly reduce greenhouse gas emissions, while controls, which received no biochar addition, showed no statistically significant effect on greenhouse gas emissions, demonstrating that while biochar addition to soil may mitigate greenhouse gases, it is not linearly correlated (Verheijen et al., 2010). Woolf et al (2010), recommended a global biochar application rate of 50 Mg ha^{-1} in most agricultural systems, generating mean yield increases of ~18%. Jeffery et al (2010) observed that biochar application to soil

resulted in greenhouse gas sequestration, which on average, were associated with biochar applications at rates higher than 5 Mg ha^{-1}.

Addition of biochars to low erosion soils has been associated with decreased soil C mineralization, also referred to as negative priming, (Francisco et al., 2015). This contrasts with previous research indicating that negative priming is more likely in long incubations with biochars made at high pyrolysis temperatures and from hardwood feedstock (Zimmerman et al., 2011). Research by others have shown that biochar C mineralization potential tends to decrease with increasing pyrolysis temperature (Bruun et al., 2008), possibly because of formation of recalcitrant aromatic C compounds (Rutherford, 2012). Wang et al (2014) found that compared to the bamboo leaf feedstock, biochar addition to soil resulted in higher organic C storage and attributed the biochar's effect to a reduced impact on microbial feedstock, dissolved organic C and CO_2 fluxes relative to the feedstock. Wu et al (2013) compared wheat straw feedstock with its biochar and found that comparatively up to 77% of the uncharred straw C was lost as CO_2 upon incubation, with the increased C loss from uncharred straw attributed to the higher dehydrogenase and β-glucosidase content of straw-amended soils relative to biochar-amended soils. Francisco et al (2015) found that charring feedstock at 500^{o}C, then amending soil with it results in a net sequestration of C; although pyrolysis causes a mass loss of ~70% of the feedstock C, the 500^{o}C char can reach nearly four times the C sequestration efficiency of the uncharred stalks.

Despite significant loss of labile N by volatilization on heating (70-90%) to prepare the biochar, biochar residues can contain considerable amounts of N (Wang et al., 2012). However, only a small portion of this N can be directly released to the soil N pool (Rajkovich et al., 2012), at a rate determined by the production variables of the biochar

(Rajkovich et al., 2009) since most of the N in biochar is heterocyclic forms (Jeffery et al., 2012). Biochar can reduce soil N losses, such as soil N_2O emissions, NH_3 volatilization and N leaching (Taghizadeh-Toosi et al., 2012), so that the net outcome of its addition is assumed to be higher N-use efficiency.

Labile C compounds usually present on the surface of biochars, despite their recalcitrant C structure, may cause initial N-immobilization when the biochar is applied to soil resulting in a decrease of foliar tissue N in crops, (Jeffery et al., 2010; Rajkovich et al., 2012). Addition of a complementary source of N (mineral or organic) when incorporating biochar in soil can be a management strategy to overcome this problem (Abalos et al., 2013). Research results on the effects of biochar applications on soil mineral N have been varied. Biochars can reduce soil N available to plants both by microbial immobilization and by absorption of soil mineral N (Yao et al., 2012; Zheng et al., 2013). Miller et al (2011) found that hardwood biochar can produce elevated rhizosphere NO_3.

Biochars have been observed to be effective in sequestering greenhouse gases (GHG) such as CO_2, CH_4 and N_2O (Lehmann et al., 2008) when employed as a soil amendment. Early research was conducted on soils found in the Terra Preta region of the Amazon rainforest, where indigenous communities employed the charring of feedstock technique as a way to improve soil fertility (Glaser et al., 2001, 2002). Recent extensive research on the use of biochar as a soil amendment has shown increased carbon sequestration in soils amended with biochar, including reduced leaching of N into ground water, reduced N_2O emissions, improved soil fertility due to increased cation-exchange capacity and a large surface area that promotes higher soil microbial activity (Glaser et al., 2001, 2002; Lal et al., 2004; Lehmann et al., 2006; Yamato et al., 2006; Lal et al.,

2007; Chan et al; 2008; Lehmann et al., 2008; Larson et al., 2009; De Gryze et al., 2010; Matovic et al., 2011). These beneficial effects of biochars and the inexpensive process of preparation from a variety of feedstock, increases the potential to provide an additional source of revenue for small-scale producers employing agroforestry-farming practices (Yoo and Kang, 2012). The information generated from this research may assist in further assessment of the value of biochar for production by agroforestry practitioners and its potential uses for environmental management in mid-Missouri.

The objective of this research was to measure the effects of biochar added to selected soils on soil greenhouse gas flux (i.e., CO_2, N_2O and CH_4) with respect to time, temperature, pH and moisture as compared to unamended soils. Three feedstock types (i.e., walnut hulls, switchgrass and cottonwood) derived from temperate agroforestry practices and their respective biochars prepared at thermal variations (300 and 500^oC) were subjected to a 29-day laboratory incubation to determine their effect on greenhouse gas emissions when used as a soil amendment. This experiment also used previous analyses of the biochar from ^{13}C NMR and FTIR-DRIFTS spectra, data from total carbon and nitrogen (see Chapter 2) as well as information drawn from comprehensive statistical analyses of data derived from GC measurements of headspace gases to draw relationships between greenhouse gas emissions and the feedstock/biochar chemical characteristics.

MATERIALS AND METHODS

Soils and Biochar

Bulk soil from the 0 to 15 cm depth of a cultivated row crop floodplain field located at the Horticulture and Agroforestry Research Center (HARC) in New Franklin, Missouri, U.S.A (39.007491, -92.750505) was collected on October 5th, 2015 (Figure 3.1). The floodplain soil was classified as the Nodaway Series (fine-silty, mixed,

superactive, nonacid, mesic Mollic Udifluvents). This soil is very deep, moderately well drained and formed in alluvium. The collected soil was then air-dried and ground using a hammer mill to pass a stainless-steel sieve with 2 mm openings. Soil chemical and physical properties were determined on three subsamples taken from the bulk soil using standard analytical procedures described by Nathan et al. (2006) at the University of Missouri Soil and Plant Testing Laboratory.

A total of three different biochars derived from walnut (*Juglans regia*) hulls, switchgrass (*Panicum virgatum*) and cottonwood (*Populus deltoids*) feedstock from the University of Missouri-Columbia Horticulture Center, were produced for the experiment. The biochar was produced in controlled anaerobic 500 ^{o}C pyrolysis reactor environments at the University of Missouri-Columbia Agricultural Engineering Laboratory. The biochars and their respective feedstock materials were then characterized using solid-state NMR and FTIR-DRIFTS technologies (See Chapter 2), to determine the labile and recalcitrant functional groups giving the biochars and feedstock their characteristic response in soil. Biochars prepared at 500^{o}C pyrolysis temperature were determine to have total carbon concentrations of >75% while those prepared at 300^{o}C have a carbon content of between 60-70% (see Chapter 2). The C/N ratios decreased at higher pyrolysis temperatures, also corroborating the finding of Cao et al., (2012) of a significant positive linear correlation in carbon content with respect to temperature. A decrease in nitrogen content with pyrolysis from ~1% in feedstock to ~0.5% for grass, hulls and woody biochars was also observed by Cao et al., (2012) in a similar observation.

Experimental Design

An incubation experiment was conducted at a controlled temperature of 35°C to assess the effects of differences in the biochar sources and soil water content on soil greenhouse gas emissions. A randomized complete block incubation experiment was used to determine the interactive effects of three feedstock types (i.e., walnut hulls, switchgrass, cottonwood) and their biochars under two soil water filled pore space (WFPS) conditions (60% and 100% WFPS) on soil nitrous oxide (N_2O), methane (CH_4) and carbon dioxide (CO_2) gas flux and cumulative emissions during the incubation period. Inorganic N was added to all soils used in the incubation at a rate of 200 mg N kg^{-1} soil in the form of reagent grade KNO_3. The incubation chamber was kept at a constant temperature of 35°C, which varied slightly downward when the chamber door was opened for gas sampling.

The biochars were sieved to <2 mm size and prepared at 500°C pyrolysis for 2 to 2.5 h. Treatments were prepared by manually uniformly mixing 1.6 kg of untreated soil with biochars from walnut hulls, switchgrass and cottonwood in buckets prior to moisture addition to achieve an approximate equivalent 50 Mg ha^{-1} application rate; respective feedstocks were also applied to match the 50 Mg ha^{-1} biochar rate (Verheijen et al., 2010; Woolf et al., 2010). The N treatment was applied by mixing reagent grade chemical compound KNO_3 with 100 mL of distilled water, which was subsequently added to all treatments including the control soils with no biochar or feedstock amendments added. The 50 Mg ha^{-1} biochar rate has been used by other researchers in previous research (Venterea et al., 2008; Spokas et al., 2009).

For all treatments, distilled water was added to the soil to bring the moisture content up to either 60 or 100% WFPS. The biochar and feedstock were applied to soil in

120 mL specimen cups and placed inside 1 L sealable mason jars to provide headspace for the samples, each of which represented an individual treatment. For both the field capacity and flooded WFPS treatments, 30 mL of N solution containing 200 mg N kg^{-1} soil (224 kg N ha^{-1} equivalent) was initially uniformly added to the soil and then more deionized water was added drop wise to make each individual treatment up to 60% or 100% WFPS. Soil water content for the two moisture levels were kept constant by frequently checking (every 2-3 days) the total weights of the samples and the jars and correcting for the deficit by adding distilled water to the soil samples.

To determine the change in concentration of the N_2O, CH_4 and CO_2 greenhouse gases evolved during incubation, 20 mL gas samples were obtained from the Mason jar headspace with a syringe. For each measurement, an ambient gas sample was included as the initial concentration for calculating the emission rate during 1 hour of enclosure. The mason jars were then capped immediately with covers that had rubber septa (NQ-704 silicone adhesive sealant), and through which the gas samples were collected at 20 and 60 minutes after chamber closure. These stoppers provided an airtight seal. After the gas sampling, the septa were removed, and the jars were left open to the ambient air.

The nine sampling times chosen during the 29-day incubation period for sampling were days 1, 2, 5, 7, 9, 12, 16, 21, and 29 after the application of treatments (USDA-ARS GRACEnet protocol for trace gas sampling). The cumulative fluxes representing the greenhouse gas emission were calculated over the whole incubation period. Soil chemical characteristics (Table 3.1) were also measured from selected representative samples before the beginning of the incubation after the treatments were applied.

For analysis, the headspace gas was transferred into an evacuated 12 mL vial (Exetainer®, Labco ltd., Ceredigion, UK). Each vial had a prefitted septum. Gas samples

were analyzed for N_2O, CH_4 and CO_2 using a GC-2014 Gas Chromatograph (Shimadzu Co., Kyoto, Japan) immediately after sampling (Chintala et al., 2014a) and also in accordance with the USDA-ARS GRACEnet protocol for trace gas sampling and analysis (Parkin et al., 2010). The Shimadzu gas chromatograph, equipped with a methanizer, flame ionization detector (FID) and an electron capture detector (ECD), was calibrated with traceable gas standards (Scotty Analyzed Gases, Air Liquide America Specialty Gases LLC, Plumsteadville, PA). Nitrogen (flow rate; 25 mL min^{-1}) was used as a carrier gas for the N_2O, CH_4 and CO_2 gases. Methane was detected by FID while N_2O was detected by ECD. The CO_2 was converted into CH_4 by the methanizer and detected by FID. Oven temperature was controlled at 55°C, and the temperatures of the ECD and the FID were set at 360°C and 230°C, respectively (Kammann et al., 2009, 2011, 2012).

The GC flow scheme followed Loftfield et al., (1997). The greenhouse gas fluxes were determined from the slope of the mixing ratio change with the three sequential samples taken at 0, 20 and 60 minutes after chamber closure. Sample sets were rejected unless they yielded a linear regression value of $R^2>0.80$ (Spokas et al., 2009). The total emissions of N_2O, CH_4 and CO_2 over the whole incubation period were sequentially accumulated from the emissions averaged on every two adjacent intervals of measurements (Zou et al., 2005; Zhang et al., 2010). Low or unsteady greenhouse gas concentrations with $R^2<0.80$ were set to zero.

$$\text{GHG Flux}=\frac{d[GHG]}{dt}\times 10^{x}\times\frac{V_{head}\times p\times 100\times M_{wt}}{R\times T}\times 10^{y}\times\frac{1}{A}$$

Equation 1: The Linear regression relative to the total soil (or soil mixture) or the ground area (incubation chamber surface) followed the Ideal Gas Law

Where;

- $\frac{d[GHG]}{dt}$ is the rate or GHG concentration change (mg L^{-1} h^{-1}; µg L^{-1} h^{-1})

- 10^x is a conversion factor ($mLm^{-3}=10^{-6}m^3m^{-3}$ or $\mu Lm^{-3}=10^{-9}m^3m^{-3}$)
- V_{head} is the volume of the mason jar chamber headspace
- p is the atmospheric pressure (hPa)
- M_{wt} is the molecular weight of the respective gas species (g mol^{-1})
- R is the universal gas constant =8.314 (J $mol^{-1}K^{-1}$)
- T is the temperature (in Kelvin)
- 10^y is a conversion factor (g in mg, 10^3 or g in μg, 10^6)
- A is the covered soil area (m^2) or soil weight (kg)

GHG fluxes were expressed as ng, μg or mg of species emitted or consumed per kg soil (mix) per 60 minutes (hour).

Data and Statistical Analyses

Statistical analysis was conducted to determine the impact of organic soil amendments and WFPS on cumulative of CO_2, N_2O and CH_4 emissions. Analysis of variance (ANOVA) was used with type of organic matter amendment and WFPS as the fixed effects and block as a random factor.

ANOVA was determined using the Generalized Linear Mixed model from the R package 'lme4' (Bates et al 2015). Where significant effects were observed, we conducted the Tukey post-hoc test and used the 'cld' function from the 'lsmeans' package in R to extract pairwise comparisons (Lenth et al., 2016). Differences were deemed significant at $p = 0.05$. However higher significant levels ($p < 0.10$) were also considered. All analyses were carried out using R version 3.5.0 (R Core Team, 2018). Results for the N_2O, CH_4 and CO_2 emissions were arithmetic means of triplicate samples.

All greenhouse gas flux was determined from the increase or decrease in concentration over time in the headspace incubation. Treatment means were calculated

from four replicates per treatment, and error bars displayed in the figures are always standard deviations. All data was expressed as means plus or minus one standard deviation. Data were log or sqrt transformed to achieve normalcy and variance homogeneity if required.

RESULTS AND DISCUSSION

Effect of Biochar on Soil Chemical Characteristics

The chemical compositions of control soils and soils amended with biomasses from switchgrass(SG), cottonwood(CW) and walnut hulls(WH) and their respective biochars are presented in Table 3.1. Addition of biochar to soil at the beginning of the incubation showed significant effects on soil chemical properties, including total N, where higher pyrolysis biochars decreased the amount of available N in the soil.

Application of biochars to soil tended to increase soil pH with an increase in pyrolysis temperature of the biochar. Addition of CW biochar resulted in the maximum observed soil pH at 6.8. Wan et al., (2014) observed an increase in soil pH with incubation time for soils amended with biochars prepared at 300^{o}C for the first 20 days of incubation. They attributed this phenomenon to soil organic nitrogen (N) mineralization. Cayuela et al., (2013), in their study of the effect of biochar on denitrification in soil, observed a direct relationship between changes in pH to denitrification and overall N_2O mitigation in soils amended with biochars.

Addition of biochar generally increased soil CEC for all treatments compared to except for SG, while change in pyrolysis temperature had fluctuating effects (Table 3.1). Wan et al., (2014) observed from measurements done for the first 20 days of incubation a significant increase in soil CEC with biochar amendment, confirming that biochars made the surface of soil more negative.

For this study, the application of biochar coincided with a linear increase in exchangeable Ca^{2+}, Mg^{2+} and K^{+} concentrations, relative to the control (Table 3.1). This compares closely to observations by Wan et al., (2014), who observed a significant increase in soil exchangeable base cations, which was especially consistent for Ca^{2+}, Mg^{2+} and K^{+} across all treatments. They also observed a drastic decrease in exchangeable Al^{3+} with increase in pyrolysis temperature from 300 to 500^{o}C, which was not included in this study.

Effect of Organic Material and WFPS on Soil N_2O Emission

The source and form of the applied organic material had no effect on soil N_2O fluxes (Fig 3.3 to 3.5). The additional N applied with the treatments may have stimulated further soil N_2O emissions thereby enabling observations of significant reductions by biochar as compared to applied feedstocks that would be a source of degradable carbon for denitrification (Beauchamp et al., 1989; Granli and Brøchmann, 1994; Burger et al., 2005; Li et al., 2005).

Effect of Organic Material and WFPS on Soil CO_2 Flux

Pyrolysis led to significant reduction in soil CO_2 fluxes only when CW was applied but at only 60% WFPS (Fig 3.3 to 3.5). At this moisture level, CWP reduced soil CO_2 flux over CW, thereby sequestering cumulative emissions by around 93% (Fig. 3.2). Compared to the control, only CW showed higher soil CO_2 emissions ($p < 0.001$). Therefore, interaction of organic material treatments and WFPS had a significant effect on soil CO_2 fluxes ($p < 0.003$) (Table 3.3).

Spokas et al., (2009) and Yanai et al., (2007) observed in their laboratory-based incubation studies, that the biochars seem to have suppressed CO_2 production. According to Chang et al., (2016), these differences were associated to the time delay between the

start of the experiment and the strong diurnal soil CO_2 emission cycles that were observed two to four days later. None of the organic soil amendments had any significant effect on cumulative CO_2 emission at 100%, whether the biochars or their respective biomasses were used or not.

Research by Brunn et al., (2008) have shown that biochar C mineralization potential tends to decrease with increasing pyrolysis temperature, possibly because of formation of recalcitrant aromatic C compounds (Rutherford, 2012). Wang et al (2014) found that compared to bamboo leaf feedstock, biochar addition to soil resulted in higher organic C storage, thereby reducing dissolved organic C and CO_2 fluxes relative to feedstock. Studies by Francisco et al (2015) found that charring feedstock at 500^{o}C, then amending soil with it results in a net sequestration of C with ~4 times the efficiency of uncharred stalks.

Effect of Organic Material and WFPS on Soil Methane Flux

Methane oxidation is very sensitive to variation in water content (Castro et al., 1994; Kamman et al., 2001). We had expected a gradual increase in soil CH_4 release at constant biochar rates and an uptake with biochar application in contrast with their feedstocks and control combinations in the treatments. As was observed by Kamman et al., (2012), CH_4 uptake was not negatively affected by biochar addition with respect to the controls.

Soil WFPS significantly affected soil CH_4 flux (Figs. 3.3 to 3.5) but at $p = 0.075$, so that increased CH_4 emissions were observed at saturated conditions.

Effect of Organic Material and WFPS on Cumulative Emissions of Greenhouse Gases

Cumulative greenhouse gas emissions was calculated from data derived from headspace gas flux measurements done on 9 sampling days for a total of 29 days of incubation (Fig. 3.6 to 3.10). Across feedstock types except for switchgrass, it was observed that increase in moisture content from 60 to 100 WFPS increased CO_2 production. Addition of biochar decreased cumulative CO_2 emissions in comparison to the control for all feedstock types. This observation was similar to findings by Case et al., (2012), who compared differences between soils amended with different amounts of biochar. They found that while correlation between biochar application rates and CO_2 emissions, there was a significant increase in CO_2 emissions with the application of biochar. Francisco et al (2015) found that amending soil with charred feedstock at 500^oC resulted in net cumulative C sequestration, while studies by Wang et al (2014) show that unpyrolyzed feedstock had higher cumulative CO_2 emissions compared to biochar addition to soil, which caused higher organic C storage.

A decrease in the net cumulative N_2O production with time was observed in all feedstock types, with moisture and addition of biochar playing an important role in determining the rate of N_2O emission (Fig. 3.6 to 3.10). Compared to the controls, for all feedstock types, addition of biochar sped up the production of N_2O until day 20. Addition of moisture to 100% WFPS also stimulated increased N_2O emission compared to the control. Case et al., (2012) made a similar observation, where headspace N_2O concentration rapidly decreased with addition of biochar. Li et al., (2005) compared correlated the additional N applied with the treatments to stimulation of further soil N_2O emissions.

The nature of organic amendment to the soil and of amendment-WFPS interaction, however, had no influence on soil CH_4 fluxes, and hence, no effect on

cumulative soil CH_4 emission. Increasing WFPS led to an approximately 26-fold increase in cumulative soil CH_4 emission in most of the treatments, especially between day 20 to 29 of incubation (Figures 3.6 to 3.10). Kamman et al., (2012) observed that CH_4 uptake was not significantly affected by biochar addition with respect to the controls. In this research, it was observed that the soil WFPS, especially saturated conditions, had a significant effect on cumulative soil CH_4 (Figs. 3.6 to 3.10), causing increased CH_4 emissions at $p = 0.075$.

Chemical Properties of the Feedstock

The three biochars derived from walnut (*Juglans regia*) hulls, switchgrass (*Panicum virgatum*) and cottonwood (*Populus deltoids*) feedstock were produced for the experiment in controlled anaerobic 500 ^oC pyrolysis reactor environments. Their chemical characteristics were obtained using solid-state NMR and FTIR-DRIFTS technologies and the results are discussed at length in Chapter 2. The labile and recalcitrant functional groups were determined to better understand the characteristic responses of biochars and their respective feedstock in soil. The C/N ratios decreased at higher pyrolysis temperatures, corroborating findings by Cao et al., (2012) of significant positive linear correlation in carbon content with respect to temperature.

CONCLUSIONS

The effects of biochar amendments on soil properties and soil GHG emissions were biochar-specific. This is probably because the community structure and activity of the soil microbial community drives the net production of greenhouse gases in the soil matrix. Furthermore, the results of short-term incubations may not be indicative of long-term (>1yr) impacts of biochar amendments, even though results from short-term incubation research indicates an advantage in converting feedstock to biochar prior to soil

incorporation for reducing soil greenhouse gas emissions shortly after application. However, additional research on this effect and the temporal duration of the reduction needs to be determined.

The laboratory incubations used in this research were conducted in the absence of multiple factors that might be encountered under field conditions including the presence of plants, earthworms, rainfall, variability in diurnal temperature, soil microbial inocula and many other factors that may have had significant effects on soil greenhouse gas emissions in the field.

Except for CO_2, biochar additions did not have significant effects on reducing soil N_2O and CH_4 emissions even with N addition and moisture variation for the duration of the incubation. The three tested biochars proved to be more stable in soil than their corresponding feedstock. Feedstock addition caused an observed significant statistical difference in CO_2 emission compared to the control, unlike the biochars which did not have significant difference in their effect to CO_2 production due their recalcitrance in the soil. One goal for future studies would be to work towards the development of a suitable guideline for standardized incubation experiments, while paying attention to the GRACEnet Protocols to screen a much broader variety of biochars as relates to soil type, moisture content and temperature and the effect on greenhouse gas sequestration potentials of the biochars.

REFERENCES

Adams LB, Hall CR, Holmes RJ, Newton RA. An examination of how exposure to humid air can result in changes in the adsorption properties of activated carbons. Carbon, 1988, 26: 451-459.

Baldock J, Smernik R. Chemical composition and bioavailability of thermally altered Pinus resinosa (Red pine) wood. Org. Geochem., 2002, 33:1093-1109.

Bridgwater AV, Bridge SA. A review of feedstock pyrolysis and pyrolysis technologies. In: Bridgwater AV, Grassi G eds. Feedstock Pyrolysis Liquids Upgrading and Utilization. London: Elsevier Science, 1991, 11-92.

Bates D, Maechler M, Bolker B. and Walker, S., 2015. lme4: Linear mixed-effects models using Eigen and S4. R package version 1.1–7. 2014.

Case SDC, McNamara NP, Reay DS, Whitaker J. The effect of biochar addition on N2O and CO2 emissions from a sandy loam soil-The role of soil aeration. Soil Biology and Biochemistry, 2012, 51:125-134

Cayuela ML, Sanchez-Monedero MA, Roig A, Hanley K, Enders A, Lehmann J., Biochar denitrification in soils: when, how much and why does biochar reduce N_2O emissions? Sci. Rep., 2013, 3:1732

Cheng CH, Lehmann J, Thies JE, Burton SD, Engelhard MH. Oxidation of black carbon by biotic and abiotic processes. Org. Geochem., 2006, 37: 1477-1488.

Demirbas A. Feedstock resources for energy and chemical industry. Energy Edu. Sci. Technol., 2000, 5: 21-45.

El-Hendawy ANA, Samra SE, Girgis BS. Adsorption characteristics of activated carbons obtained from corncobs. Coll. Surf. A: Physicochem. Eng. Aspects, 2001, 180:209-221.

Firestone MK, Firestone RB, Tiedje JM. Nitrous oxide from soil denitrification: Factors controlling its biological production. Science, 1980, 208: 749-751.

Glaser B, Haumaier L, Guggenberger G, Zech W., The 'Terra Preta' phenomenon: a model for sustainable agriculture in the humid tropics. Naturwiss., 2001, 88: 3741.

Guerro M, Ruzi MP, Alzuet MU, Bilbao R, Miller A. Pyrolysis of eucalyptus at different heating rates: studies of char characterization and oxidative reactivity. J. Anal. Appl. Pyrolysis, 2005, 74: 307-314.

Huang Y, Zou J, Zheng X, Wang Y, Xu X. Nitrous oxide emission as influenced by amendment of plant residues with different C:N ratios. Soil Biol. Biochem., 2004, 36: 973-981.

Karagoz S, Bhaskar T, Muto A, Sakata Y. Comparative studies of oil compositions produced from sawdust, rice husk, lignin and cellulose by hydrothermal treatment. Fuel, 2005, 84: 875-884.

Kawamoto K, Ishimaru K, Imamura Y. Reactivity of wood charcoal with ozone. J. Wood Sci., 2005, 51: 66-72.

Khin KM, Toyota K. Suppression of nitrous oxide production by the herbicides glyphosate and propanil in soils supplied with organic matter. Soil Sci. Plant Nutrit., 2007, 53: 441-447.

Kinney CA, Mandernack KW, Mosier AR. Laboratory investigations into the effects of the pesticides mancozeb, chlorothalonil, and prosulfuron on nitrous oxide and nitric oxide production in fertilized soil. Soil Biol. Biochem., 2005, 37: 837-850.

Laird DA. The charcoal vision: A win–win–win scenario for simultaneously producing bioenergy, permanently sequestering carbon, while improving soil and water quality. Agronomy J., 2008, 100: 178-181.

Lenth, R.V., 2016. Least-squares means: the R package lsmeans. Journal of statistical software, 69(1), pp.1-33.

Liang B, Lehmann J, Solomon D, Sohi S, Thies JE, Skjemstad JO, Luizão FJ, Engelhard MH, Neves EG, Wirick S. Stability of feedstock-derived black carbon in soils. Geochim. Cosmochim. Acta, 2008, 72: 6096-6078.

Mosier AR. Soil processes and global change. Biol. Fertil. Soils, 1998, 27: 221-229.

Murage E W, Voroney P, Beyaert RP. Turnover of carbon in the free light fraction with and without charcoal as determined using the 13C natural abundance method. Geoderma, 2007, 138: 133-143.

Nathan, M., J. Stecker, and Y. Sun. 2006. Soil testing in Missouri: A guide for conducting soil tests in Missouri. Division of Plant Sciences, College of Agriculture, Food and Natural Resources, University of Missouri. Columbia, MO.

R Core Team (2018). R: A language and environment for statistical computing. R Foundation for Statistical Computing, Vienna, Austria. URL https://www.R-project.org/.

Rondon M, Ramirez JA, Lehmann J. Charcoal additions reduce net emissions of greenhouse gases to the atmosphere. In: Proceedings of the 3rd USDA Symposium on Greenhouse Gases and Carbon Sequestration in Agriculture and Forestry, 2005 Mar 21–24; Baltimore, MD: University of Delaware Press, 208.

Rondon MA, Molina D, Hurtado M, Ramirez J, Lehmann J, Major J, Amezquita E. Enhancing the productivity of crops and grasses while reducing greenhouse gas

emissions through bio-char amendments to unfertile tropical soils. Presentation at the 18th World Congress of Soil Science, Philadelphia, PA, July 9-15, 2006, Presentation #138-68.

Schmidt MWI, Noack AG. Black carbon in soils and sediments: analysis, distribution, implications, and current challenges. Global Biogeochem. Cycles, 2000, 14: 777-793.

Sensöz S. Slow pyrolysis of wood barks from Pinus brutia Ten. and product compositions. Biores. Technol., 2003, 89: 307-311.

Sergides CA, Jassim JA, Chughtai AR, Smith DM. The structure of hexane soot. Part III: Ozonation studies. Appl. Spectroscopy, 2000, 41: 482-492.

Spokas KA, Koskinen WC, Baker JM, Reicosky DC. Impacts of woodchip biochar additions on greenhouse gas production and sorption/ degradation of two herbicides in a Minnesota soil. Chemosphere, 2009, 77: 574-581.

Steiner C, Teixeira WG, Lehmann J, Zech W. Microbial response to charcoal amendments of highly weathered soils and Amazonian Dark Earths in Central Amazonia – preliminary results. In: Glaser B and Woods WI eds. Amazonian Dark Earths: Explorations in Time and Space, Berlin: Springer, 2004, 195-212.

Venterea RT, Baker JM. Effects of soil physical nonuniformity on chamber-based gas flux estimates. Soil Sci. Soc. Amer. J., 2008, 72: 1410-1417.

Wan Q., Yuan JH, Xu RK, Li XH. Pyrolysis temperature influences ameliorating effects of biochars on acidic soil. Environ. Sci. Pollut. Res., 2014, 21: 2486-2495

Whitman T, Lehmann J. Biochar – one way forward for soil carbon in offset mechanisms in Africa? Environ. Sci. Policy, 2009, in press.

Yanai Y, Toyota K, Okazani M. Effects of charcoal addition on N2O emissions from soil resulting from rewetting air-dried soil in short-term laboratory experiments. Soil Sci. Plant Nutri., 2007, 53: 181-188.

Zimmerman A. Physical and chemical controls on biochar stability in the environment. Presentation at the 2009 North American Biochar Conference, Aug. 9-12, 2009. Boulder, CO.

Table 3.1. Selected soil chemical properties of the collected bulk soil and soil amended with biochar.

Material	Pyrolysis Temp.	pHs (H_2O)	Neutralizable acidity	Soil organic matter	Bray 1P	Exchangeable			CEC	Inorganic	
						Ca	Mg	K		NH_4^+-N	NO_3^--N
			$cmol_c\ kg^{-1}$	$g\ kg^{-1}$	---------- $mg\ kg^{-1}$ ----------				$cmol_c\ kg^{-1}$	---------- $mg\ kg^{-1}$ ---------	
SG†	300°C	5.8 ± 0.2††	2.1 ± 0.4	17.3 ± 0.3	26.1 ± 1.5	1689 ± 21	277 ± 17	217 ± 7	14.5 ± 0.8	2.95 ± 0.15	7.00 ± 0.22
	500°C	6.2 ± 0.2	2.3 ± 0.2	16.8 ± 0.8	27.3 ±0.3	1736 ± 26	270 ± 24	201 ± 23	13.6 ± 1.7	3.25 ± 0.15	6.77 ± 0.45
WH†	300°C	6.2 ± 0.2	2.5 ± 0.0	18.1 ± 0.5	26.3 ± 1.3	1740 ± 30	275 ± 19	213 ± 11	15.7 ± 0.4	3.00 ± 0.10	7.31 ± 0.09
	500°C	6.4 ± 0.3	2.2 ± 0.1	17.1 ± 0.5	27.5 ± 1.1	1643 ± 20	280 ± 22	208 ± 09	15.0 ± 0.8	3.17 ± 0.13	6.71 ± 0.29
CW†	300°C	6.3 ± 0.2	2.4 ± 0.2	18.5 ± 0.6	26.6 ± 1.4	1778 ± 36	279 ± 14	210 ± 13	15.4 ± 0.7	3.40 ± 0.14	7.38 ± 0.10
	500°C	6.8 ± 0.1	2.1 ± 0.2	18.1 ± 0.7	27.9 ± 1.6	1752 ± 32	288 ± 27	215 ± 17	14.0 ± 0.5	3.55 ± 0.19	7.51 ± 0.22
Control	0°C	5.6 ± 0.1	2.5 ± 0.5	18.9 ± 0.2	26.3 ± 2.3	1700 ± 173	268 ± 45	218 ± 0	15.7 ± 0.8	3.11 ± 0.14	7.11 ± 0.16

†SG, WH and CW refers to switchgrass, walnut hulls and cottonwood biochars, respectively, prepared at 300°C and 500°C pyrolysis temperatures. Control is the untreated soil. ††Mean ± 1 standard deviation

Table 3.2. Chemical properties (pH, total C, total N and C/N ratios) of switchgrass, cottonwood and walnut hulls feedstock and their respective biochars prepared at 300°C and 500°C pyrolysis temperatures.

Property/ Statistic	Switchgrass (SG)			Cottonwood (CW)			Walnut Hulls (WH)		
	Feedstock†	300°C	500°C	Feedstock	300°C	500°C	Feedstock	300°C	500°C
pH (H_2O)	5.21±0.10††	8.23±0.10	11.12±0.12	5.33±0.11	7.89±0.10	10.91±0.11	5.42±0.13	7.95±0.10	10.78±0.10
Total C (%)	50.95 ± 0.26	71.29 ± 0.44	75.88 ± 0.42	49.08 ± 0.04	65.97 ± 0.09	72.84 ± 0.53	47.54 ± 0.15	62.01 ± 0.30	63.06 ± 0.38
Total N (%)	0.88 ± 0.02	1.58 ± 0.01	1.87 ± 0.01	0.53 ±0.00	1.93 ± 0.00	1.04 ± 0.01	1.12 ± 0.01	1.89 ± 0.01	1.87 ± 0.04
C/N Ratio	58.20 ± 0.02	45.63 ± 0.01	40.64 ± 0.00	92.05 ± 0.01	34.18 ± 0.00	69.79 ± 0.01	42.62 ± 0.01	32.87 ± 0.00	33.75 ± 0.02

†Feedstock refers to original plant materials and 300 and 500 refers to biochars prepared at 300 °C and 500 °C pyrolysis temperatures, respectively. ††Mean ± 1 standard deviation

Table 3.3. Cumulative CH_4 (mg $m^{-3}h^{-1}$), CO_2 (mg $m^{-3}h^{-1}$) and N_2O (mg $m^{-3}h^{-1}$) emission from soils treated with non-pyrolyzed material (Cottonwood (CW), Switchgrass (SG) and Walnut Hulls (WH)), and pyrolyzed material Cottonwood (CWP), Switchgrass (SGP) Walnut Hulls (WHP)) at 60% and 100% water filled pore spaces (WFPS)

		Greenhouse gas								
		CH_4			CO_2			N_2O		
Treatments	Organic material	60	100	Mean†	60	100	Mean	60	100	mean
Non-pyrolized	CO	0.15 (1.69)^{a}	0.82 (36.83)^{a}	0.49 (0.24) ^{A}	203.44 (294.62)^{bc}	211.97 (151.2)^{bc}	207.71 (0.24)^{D}	8.34 (2.81)^{a}	1.07 (0.88)^{a}	4.71 (0.24)^{A}
	CW	5.23 (0.08)^{a}	53.51 (0.44)^{a}	29.37 (23.31)^{A}	1606.51 (99.75)^{a}	489.99 (36.36)^{bc}	1048.25 (23.31)^{A}	0.22 (4.02)^{a}	1.99 (0.69)^{a}	1.11 (23.31)^{A}
	SG	0.98 (0.08)^{a}	90.57 (0.08)^{a}	45.78 (43.23)^{A}	706.19 (35.64)^{bc}	830.81 (67.63)^{b}	768.5 (43.23)^{AB}	0.86 (1.54)^{a}	0.68 (1.03)^{a}	0.77 (43.23)^{A}
	WH	0.06 (0.02)^{a}	35.42 (0.11)^{a}	17.74 (8.76)^{A}	812.33 (173.29)^{b}	453.98 (25.24)^{bc}	633.16 (8.76)^{BC}	7.3 (1.57)^{a}	1.79 (0.27)^{a}	4.55 (8.76)^{A}
Pyrolized	CWP	0.1 (4.25)^{a}	0.18 (46.15)^{a}	0.14 (0.05)^{A}	109.98 (354.74)^{c}	239.62 (219.71)^{bc}	174.8 (0.05)^{CD}	7.09 (0.16)^{a}	4.09 (1.26)^{a}	5.59 (0.05)^{A}
	SGP	0.03 (0.43)^{a}	0.16 (85.93)^{a}	0.1 (0.06)^{A}	319.84 (194.9)^{bc}	184 (160.36)^{bc}	251.92 (0.06)^{CD}	6.21 (0.7)^{a}	1.05 (0.28)^{a}	3.63 (0.06)^{A}
	WHP	0.06 (0.02)^{a}	0.43 (12.23)^{a}	0.25 (0.13)^{A}	270.12 (158.69)^{bc}	325.03 (84.53)^{bc}	297.58 (0.13)^{D}	4.61 (5.21)^{a}	1.03 (0.9)^{a}	2.82 (0.13)^{A}
Mean††		0.94 (0.64)^{A}	25.87 (13.92)^{A}		575.49 (111.35)^{A}	390.77 (57.15)^{B}		4.95 (1.06)^{A}	1.67 (0.33)^{B}	
ANOVA	Organic material		p = 0.418			p < 0.001			p = 0.163	
	WFPS		p = 0.075			p < 0.034			p < 0.001	
	Organic material * WFPS		p = 0.484			p = 0.003			p = 0.327	

†Within rows, means followed by different letters in superscript are significantly different at $p < 0.05$. Lowercase letters indicate the differences including all treatment factors (organic treatment * WFPS), while uppercase letters indicate significant differences when either organic amendment (columns) or WFPS (rows) are aggregated.

††Means were separated based on Tukey's honest significant difference (HSD) test.

Numbers in brackets indicate standard error.

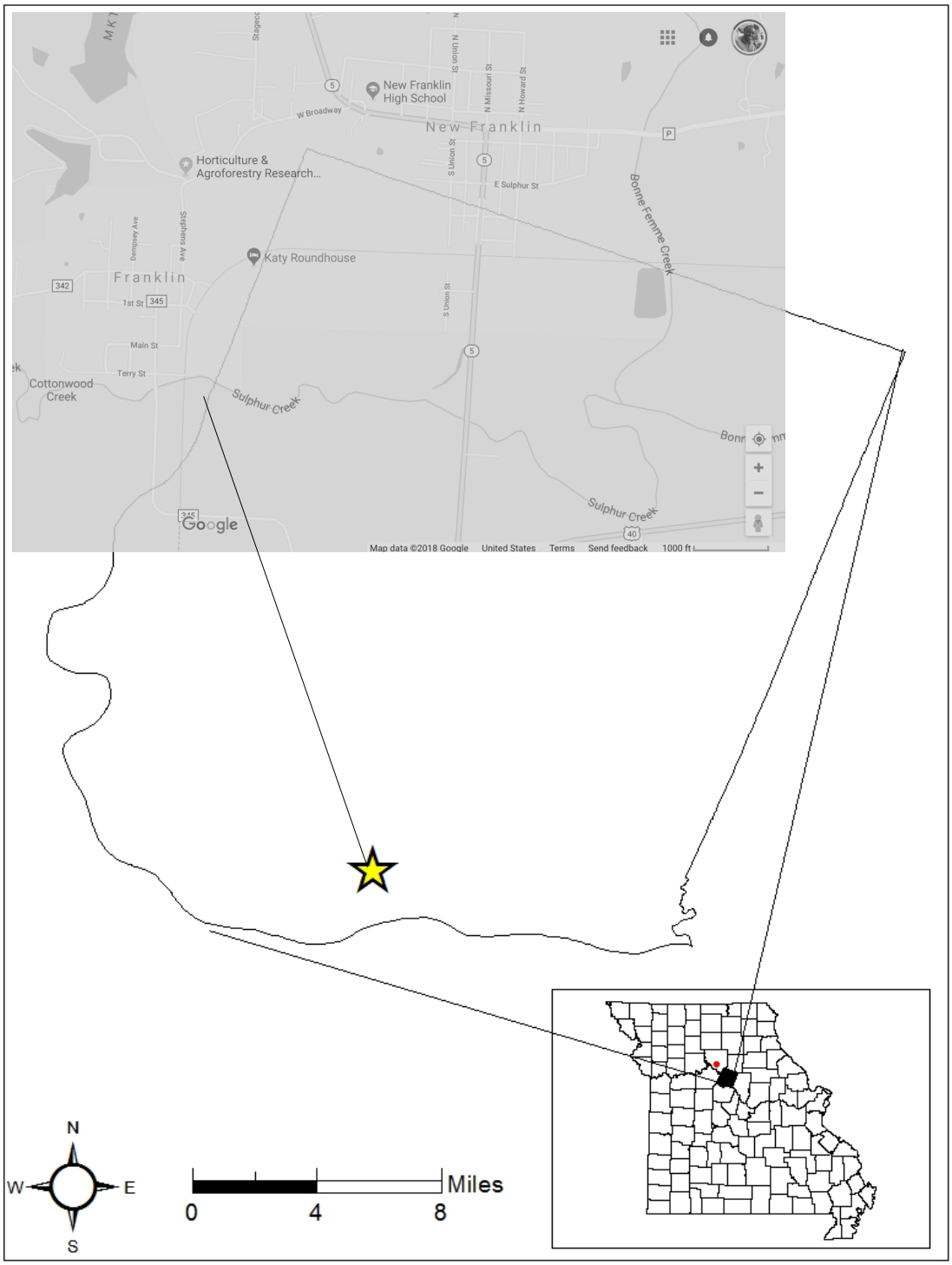

Figure 3.1. Sampling location at HARC in New Franklin, Howard County relative to the State of Missouri, United States.

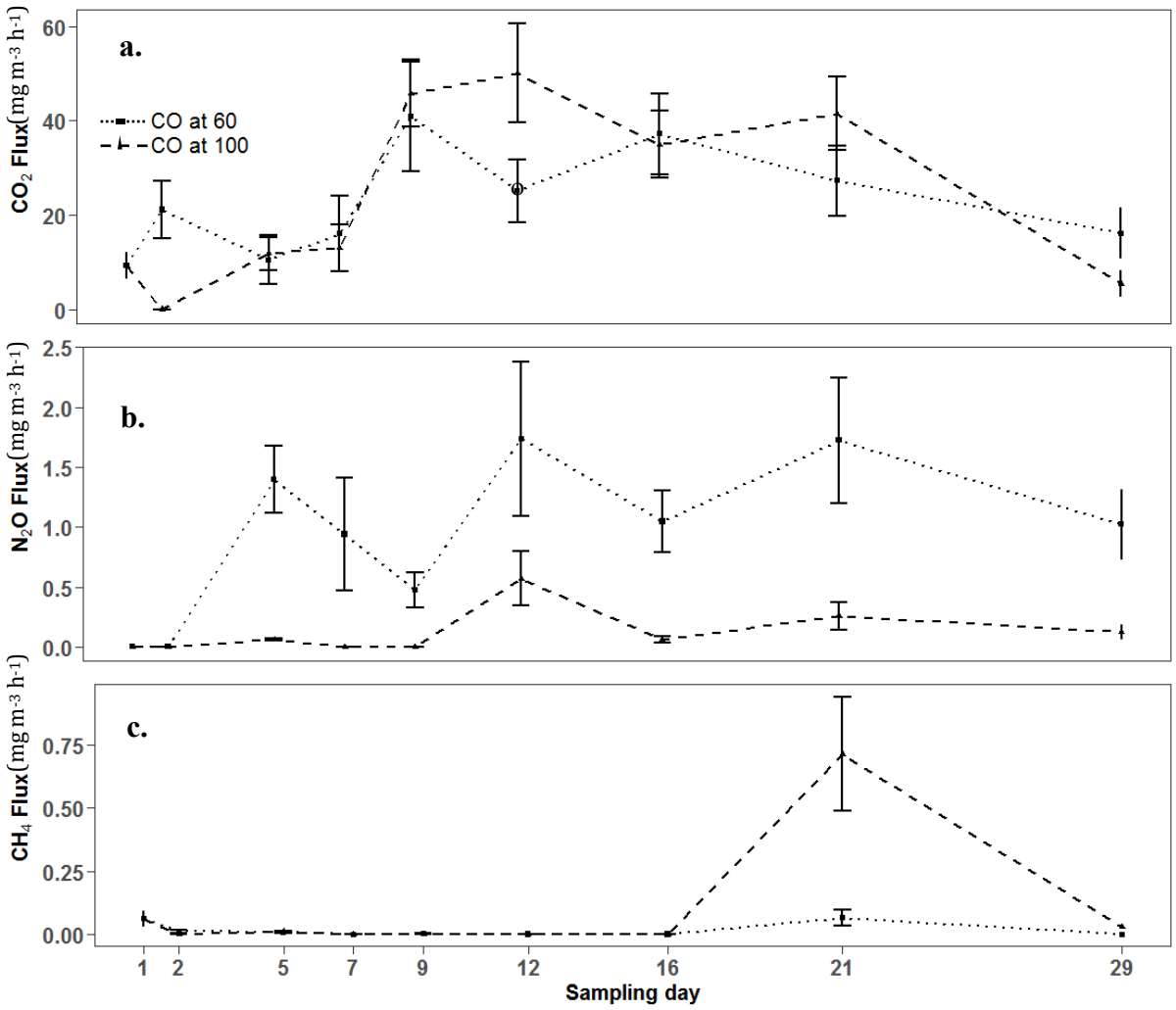

Figure 3.2: Gas flux times series for control (CO) soils of (a) Carbon dioxide (mg $m^{-3}h^{-1}$), (b) Nitrous oxide (mg $m^{-3}h^{-1}$) emission and (c) CH_4 (mg $m^{-3}h^{-1}$) from soils different organic amendments under two different moisture (WFPS) conditions. Different line symbols represent the feedstock (dotted lines are control-no feedstock), different line types show whether pyrolyzed or non-pyrolyzed, while shading shows the WFPS (60% or 100%). Dotted lines represent non-pyrolyzed at 60 WFPS; dashed, non-pyrolized at 100 WFPS; long dash, pyrolyzed at 60 WFPS; solid, pyrolyzed at 100 WFPS.

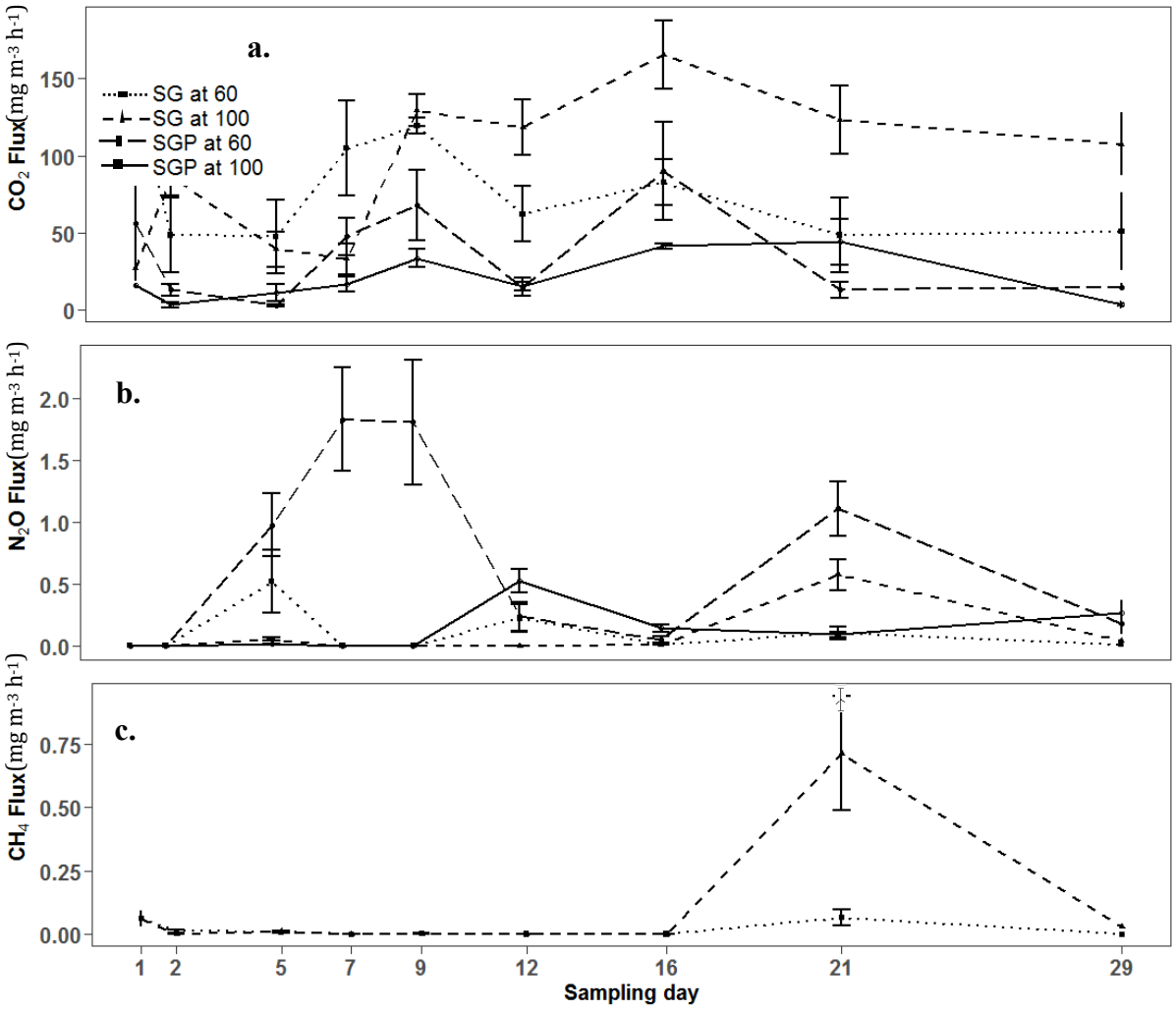

Figure 3.3: Switchgrass (SG) gas flux times series of (a) Carbon dioxide ($mgm^{-3}h^{-1}$), (b) Nitrous oxide ($mg\ m^{-3}h^{-1}$) emission and (c) CH_4 ($mg\ m^{-3}h^{-1}$) from soils different organic amendments under two different moisture (WFPS) conditions. Different line symbols represent the feedstock (dotted lines are control-no feedstock), different line types show whether pyrolyzed or non-pyrolyzed, while shading shows the WFPS (60% or 100%). Dotted lines represent non-pyrolyzed at 60 WFPS; dashed, non-pyrolized at 100 WFPS; long dash, pyrolyzed at 60 WFPS; solid, pyrolyzed at 100 WFPS.

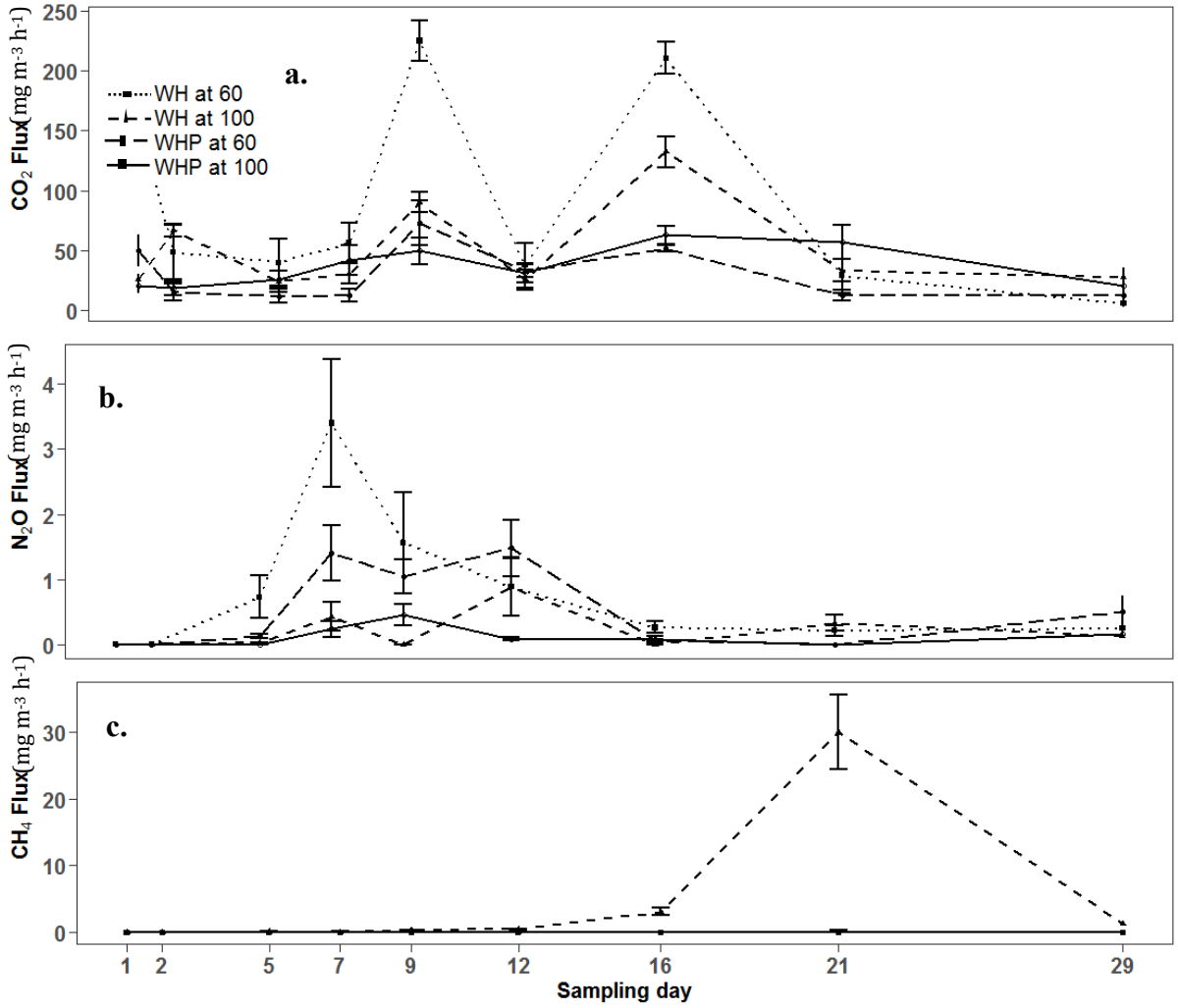

Figure 3.4: Walnut hull (WH) gas flux times series of (a) Carbon dioxide (mg $m^{-3}h^{-1}$), (b) Nitrous oxide (mg $m^{-3}h^{-1}$) emission and (c) CH_4 (mg $m^{-3}h^{-1}$) from soils different organic amendments under two different moisture (WFPS) conditions. Different line symbols represent the feedstock (dotted lines are control-no feedstock), different line types show whether pyrolyzed or non-pyrolyzed, while shading shows the WFPS (60% or 100%). Dotted lines represent non-pyrolyzed at 60 WFPS; dashed, non-pyrolized at 100 WFPS; long dash, pyrolyzed at 60 WFPS; solid, pyrolyzed at 100 WFPS.

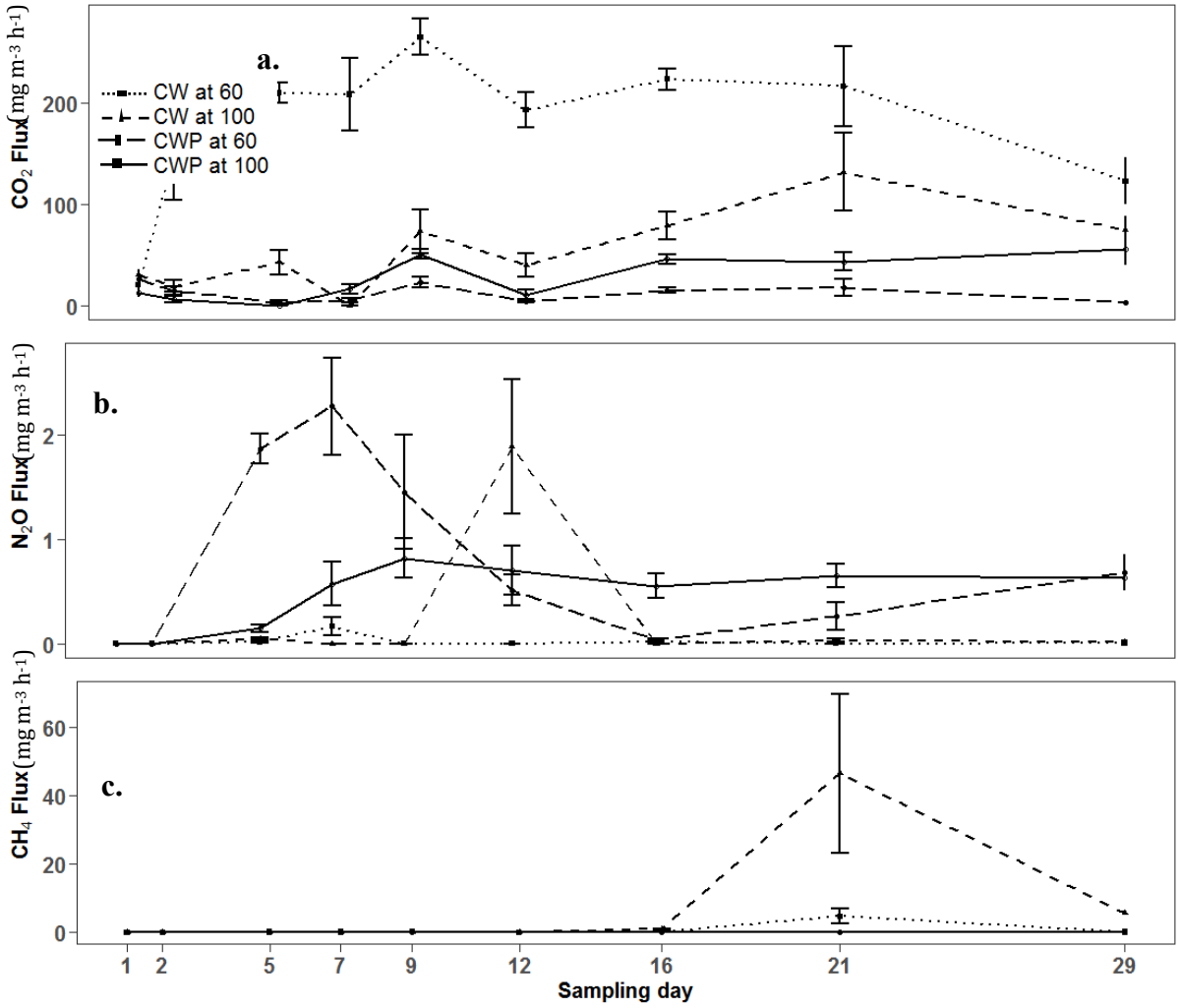

Figure 3.5: Cottonwood (CW) gas flux times series of (a) Carbon dioxide (mg $m^{-3}h^{-1}$), (b) Nitrous oxide (mg $m^{-3}h^{-1}$) emission and (c) CH_4 (mg $m^{-3}h^{-1}$) from soils different organic amendments under two different moisture (WFPS) conditions. Different line symbols represent the feedstock (dotted lines are control-no feedstock), different line types show whether pyrolyzed or non-pyrolyzed, while shading shows the WFPS (60% or 100%). Dotted lines represent non-pyrolyzed at 60 WFPS; dashed, non-pyrolized at 100 WFPS; long dash, pyrolyzed at 60 WFPS; solid, pyrolyzed at 100 WFPS.

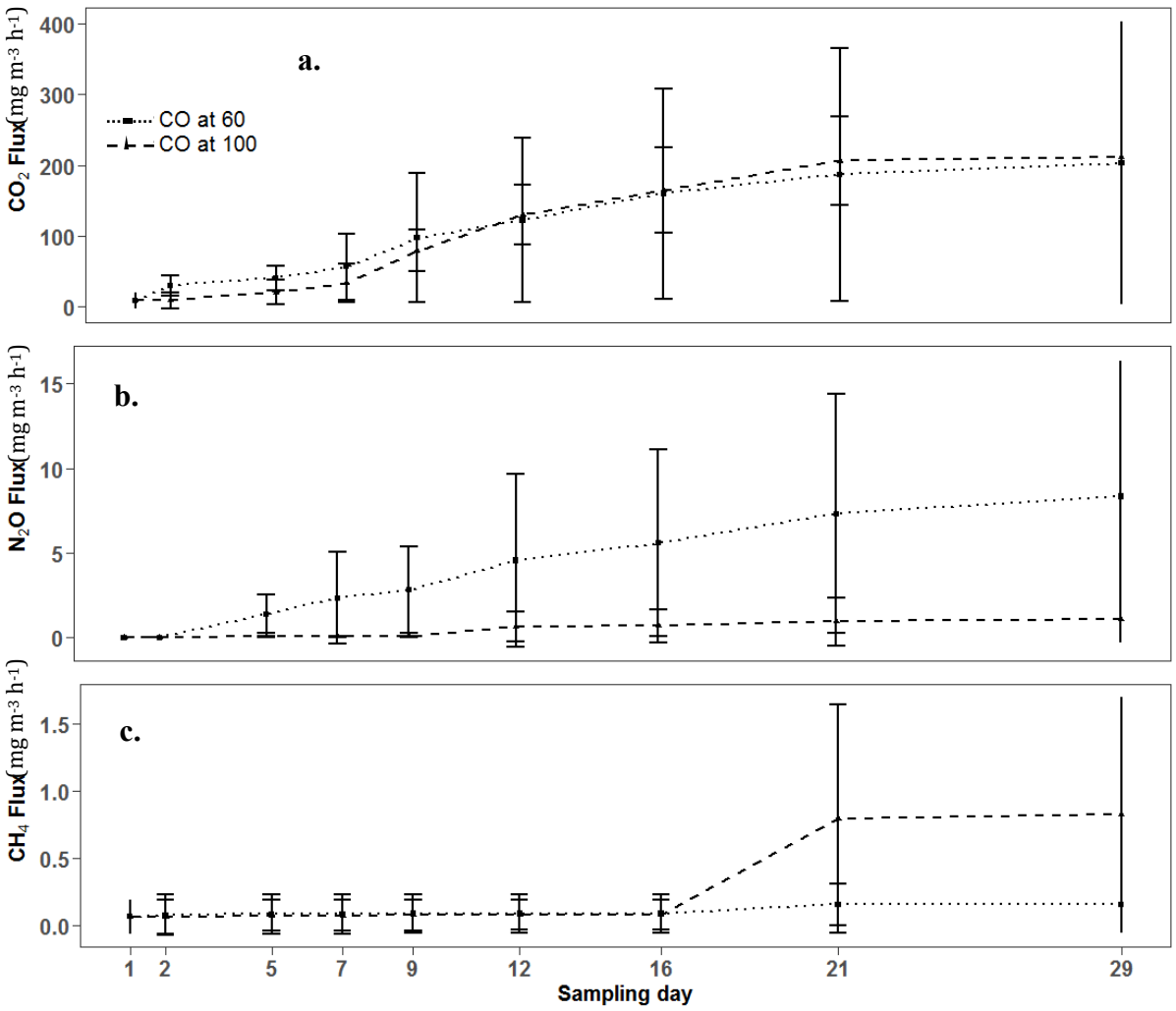

Figure 3.6: Cumulative emissions from control soils of (a) Carbon dioxide ($mgm^{-3}h^{-1}$), (b) Nitrous oxide ($mgm^{-3}h^{-1}$) emission and (c) CH_4 (mg $m^{-3}h^{-1}$) from soils different organic amendments under two different moisture (WFPS) conditions. Different line symbols represent the feedstock (dotted lines are control-no feedstock), different line types show whether pyrolyzed or non-pyrolyzed, while shading shows the WFPS (60% or 100%). Dotted lines represent non-pyrolyzed at 60 WFPS; dashed, non-pyrolized at 100 WFPS; long dash, pyrolyzed at 60 WFPS; solid, pyrolyzed at 100 WFPS.

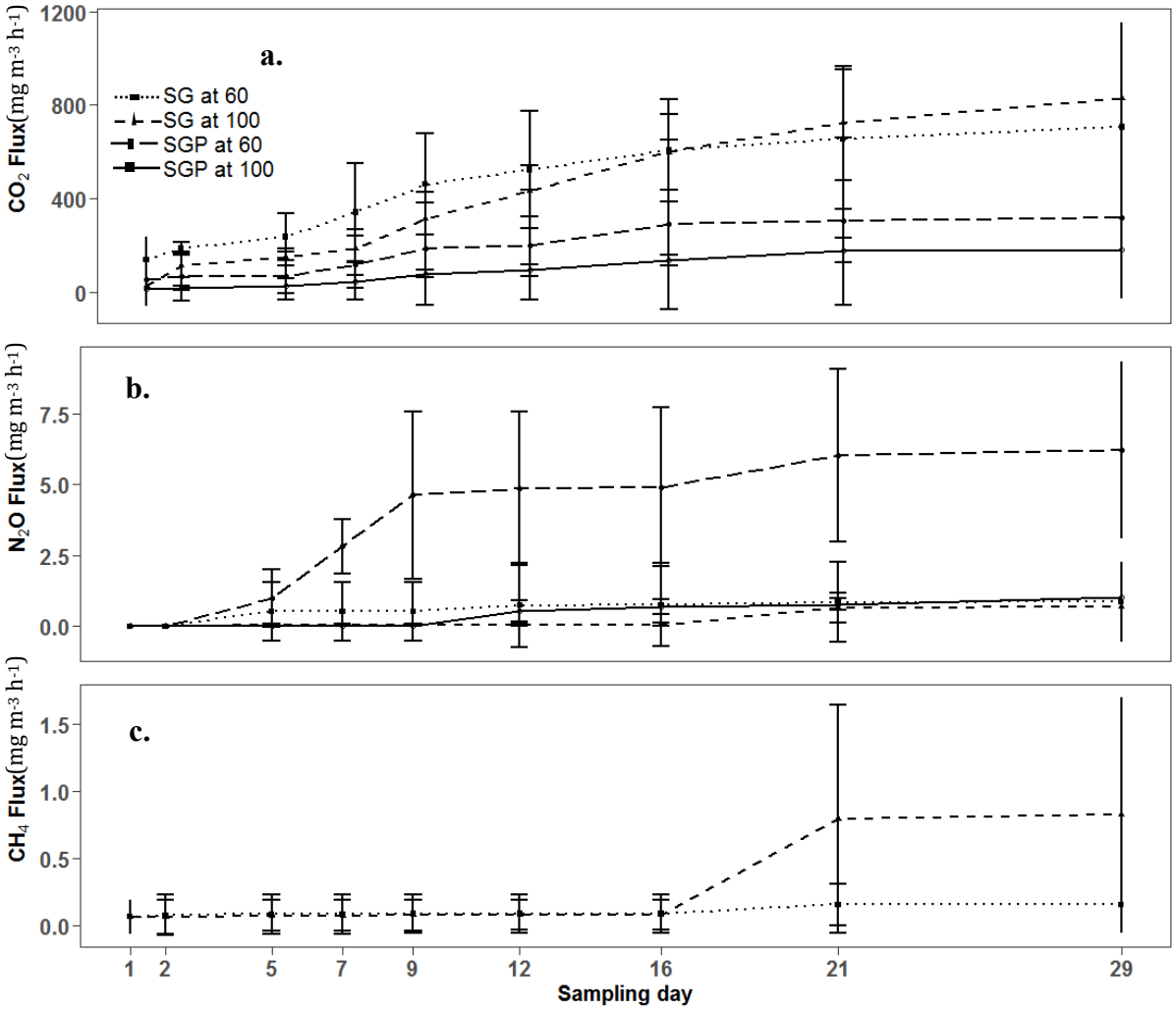

Figure 3.7: Cumulative emissions from soils treated with SG of (a) Carbon dioxide (mg $m^{-3}h^{-1}$), (b) Nitrous oxide (mg $m^{-3}h^{-1}$) emission and (c) CH_4 (mg $m^{-3}h^{-1}$) from soils different organic amendments under two different moisture (WFPS) conditions. Different line symbols represent the feedstock (dotted lines are control-no feedstock), different line types show whether pyrolyzed or non-pyrolyzed, while shading shows the WFPS (60% or 100%). Dotted lines represent non-pyrolyzed at 60 WFPS; dashed, non-pyrolized at 100 WFPS; long dash, pyrolyzed at 60 WFPS; solid, pyrolyzed at 100 WFPS.

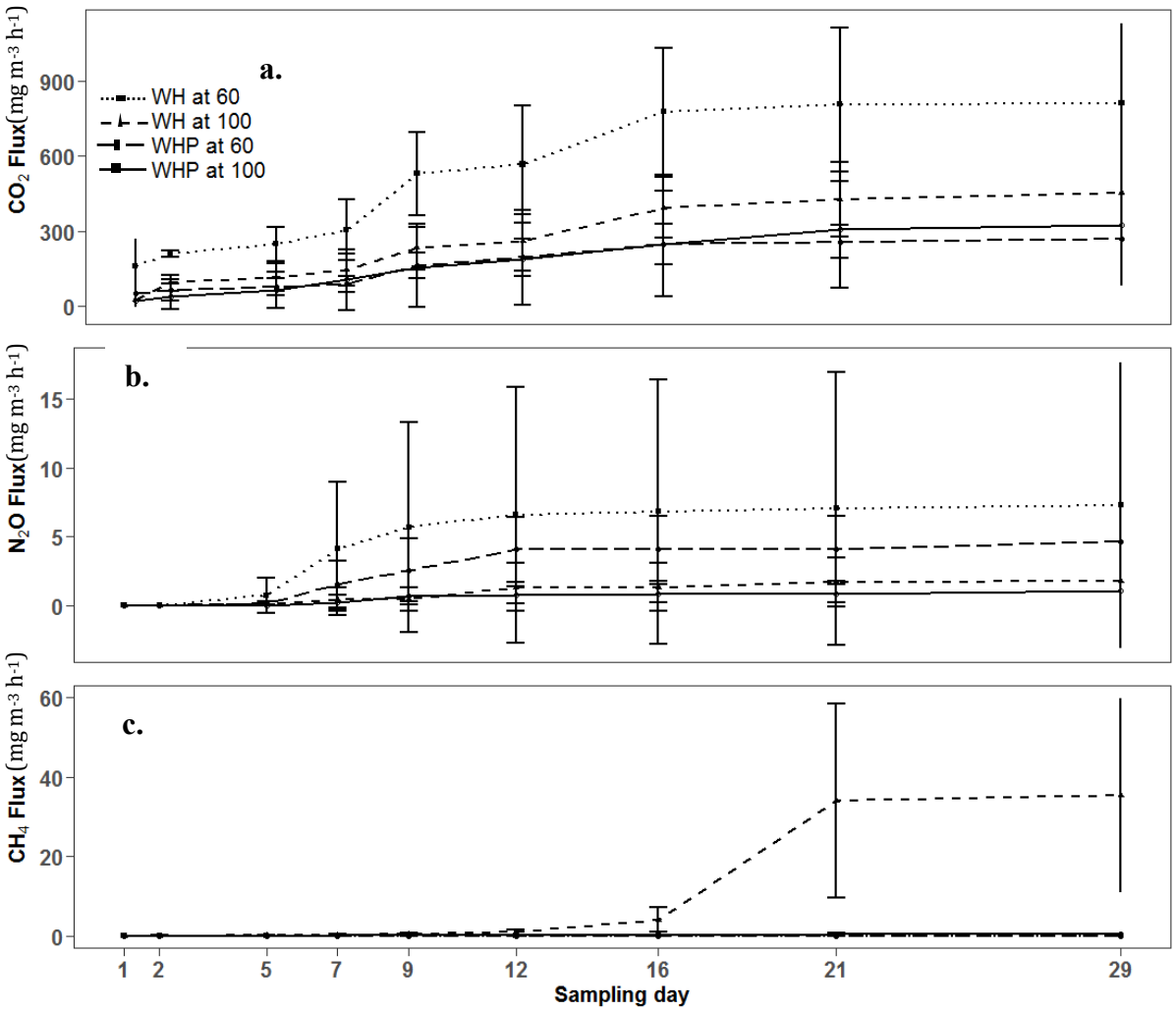

Figure 3.8: Cumulative emissions from soils treated with WH of (a) Carbon dioxide (mg $m^{-3}h^{-1}$), (b) Nitrous oxide (mg $m^{-3}h^{-1}$) emission and (c) CH_4 (mg $m^{-3}h^{-1}$) from soils different organic amendments under two different moisture (WFPS) conditions. Different line symbols represent the feedstock (dotted lines are control-no feedstock), different line types show whether pyrolyzed or non-pyrolyzed, while shading shows the WFPS (60% or 100%). Dotted lines represent non-pyrolyzed at 60 WFPS; dashed, non-pyrolized at 100 WFPS; long dash, pyrolyzed at 60 WFPS; solid, pyrolyzed at 100 WFPS.

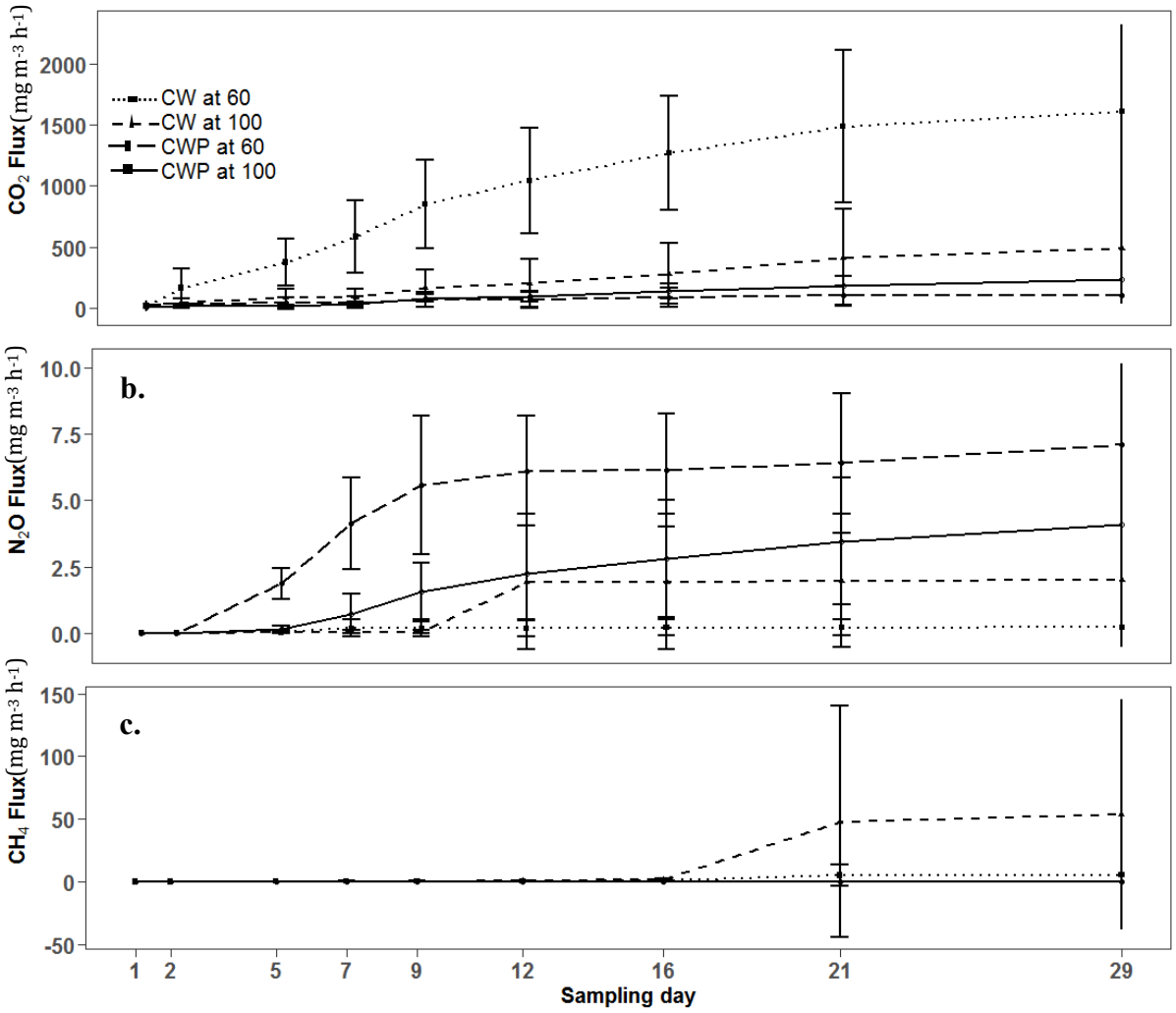

Figure 3.9: Cumulative emissions from soils treated with CW of (a) Carbon dioxide (mg $m^{-3}h^{-1}$), (b) Nitrous oxide (mg $m^{-3}h^{-1}$) emission and (c) CH_4 (m $gm^{-3}h^{-1}$) from soils different organic amendments under two different moisture (WFPS) conditions. Different line symbols represent the feedstock (dotted lines are control-no feedstock), different line types show whether pyrolyzed or non-pyrolyzed, while shading shows the WFPS (60% or 100%). Dotted lines represent non-pyrolyzed at 60 WFPS; dashed, non-pyrolized at 100 WFPS; long dash, pyrolyzed at 60 WFPS; solid, pyrolyzed at 100 WFPS.

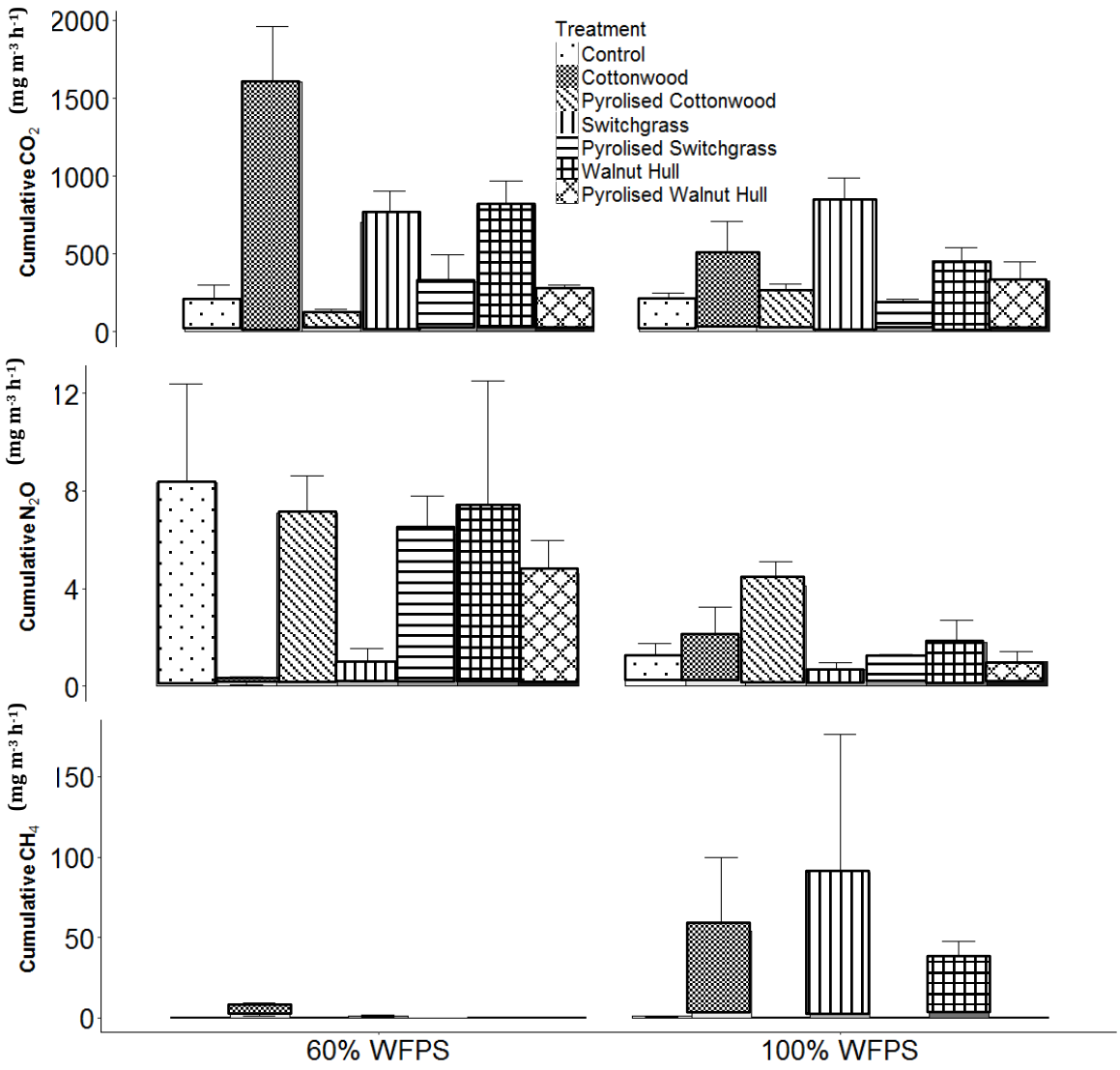

Figure 3.10. The histograms represent total CO_2, N_2O and CH_4 emissions (mg $m^{-3}h^{-1}$) from soils amended with biochars and their feedstocks for the entire 29-day incubation period. The graphs compare total emissions in soils with moisture at field capacity (60%WFPS) and flooded (100%WFPS), indicating that emissions were higher for CO_2 and N_2O at field capacity, but increased emissions for CH_4 at soil saturated conditions.

CHAPTER 4

OVERALL CONCLUSIONS

Among several driving factors affecting the characteristics of biochar, subjecting organic feedstock to high temperature pyrolysis results in multiple physical and chemical transformations. The results from this research using advanced ^{13}C NMR spectroscopic characterization of switchgrass, walnut hulls and cottonwood biochars and their respective feedstocks (with CP-TOSS magic angle spinning to enhance spectra) provide evidence of the conversion of ligno-cellulosic features during pyrolysis to more predominantly aromatic characteristics. Analyses of spectra from FTIR-DRIFTS spectroscopy results from elemental carbon and nitrogen determination corroborated conclusions from previous research with different feedstock that (i) there was a decrease in the protonated aromatic carbon and C-O functional groups during pyrolysis between 300-500 ^{O}C (ii) an enrichment of nonprotonated aromatic functional groups occurred with increase in pyrolysis temperature (iii) 300 ^{O}C pyrolysis biochars exhibited decreased ligno-cellulosic characteristics (iv) loss and disappearance of lignin, cellulose and other labile biopolymers and carbohydrates with a concurrent increase in aromatic functional groups at 500^{o}C pyrolysis temperature resulted in the biochars' acquisition of their recalcitrance.

^{13}C NMR signals from functional groups of interest yielded results that confirmed the presence of: (1) 173ppm, weak COOR/CH_3COO signals; (2) 148ppm, oxygenated aromatic C; (3) 110 - 140ppm, non-oxygenated aromatic C; (4) 103ppm, a sharp di-O-alkyl C peak; (5) 72ppm, –OCH resonating for C_4 carbons of cellulose, Cβ-carbons of cellulose and C_3 and C_5 carbons of cellulose and hemicellulose; (6) 62ppm, O-Alkyl carbon groups for $–OCH_2$ carbons and C6 carbons of cellulose; (7) 45 – 62ppm,

Methoxyl C for $ArOCH_3$ of lignin; (8) 30ppm, methylene carbons; (9) 20-0ppm, alkyl C and methyl functional groups for peaks of hemicellulose CH_3COO. These peaks cumulatively represent biopolymers in untreated feedstock including cellulose and/or hemicellulose that share chemical shifts at 62, 72, 82 and 103ppm, and lignin peaks appearing at 57, 128 and 148ppm. The similarity in the structural characteristics of our three biochar types, which possess the same dominant aromatic functional groups apparent from our ^{13}C-NMR and FTIR-DRIFTS analyses, was evidence that feedstock undergo similar thermo-chemical transformations when subjected to pyrolysis at temperatures >300 ^{o}C.

Chemical reactions that occur during high temperature pyrolysis including dehydration and condensation caused apparent depletion of total nitrogen and an increase in carbon concentration can be attributed to loss of labile N-containing ligno-cellulosic functional groups (seen in the significant reduction in the cellulose and lignin NMR/FTIR signatures) and an enrichment of aromatic compounds respectively, giving biochar its structure inherent recalcitrance. With cottonwood, switchgrass and walnut hull feedstock, the charring process would cause aromatic condensation in biochar formation. Different pyrolysis conditions, times and absence of additives, such as NaOH, during our pyrolysis could be the main factors to which we attributed differences in observations from previous research with regard to how much disappearance of labile chemical functional groups at the molecular occurred.

Our ^{13}C NMR, FTIR-DRIFTS and C/N analyses results confirmed our conclusion that the effects of biochar amendments to soil were biochar-specific, with biochar C/N ratio directly affecting the activity of soil microbial populations. More research needs to be done on the biological and biochemical processes that drive greenhouse gas

production and inhibition due to biochar application. The short-term incubation experiment results with biochar produced from switchgrass, walnut hulls and cottonwood and their respective feedstocks as soil amendments indicate a net reduction in soil greenhouse gas emissions when biochar is incorporated to the soil matrix. Conversely, addition of feedstock increased soil greenhouse gas emission, especially cumulative soil carbon dioxide emissions.

The biochars suppressed cumulative soil CO_2 emissions, while showing distinct differences in their effect on the CO_2 and N_2O/ CH_4 emission patterns and fluxes. Our biochars proved to be stable in soil due to their recalcitrance as compared to their corresponding labile feedstock because feedstock addition, unlike with biochar, caused significant statistical difference in CO_2 emission compared to the control. Moisture content variations of saturated/flooded (>100% WFPS) and field capacity (60% WFPS) did not show an effect on our greenhouse gas emissions, but we expect that in a longer incubation period >100 days, higher WFP causes higher soil N_2O-N emissions.

Additional research is necessary under standardized conditions which include such factors as more frequent greenhouse gas flux measurements, much broader variety of biochars (more than three different feedstocks and wider pyrolysis temperatures between 100 and 800^{o}C), greater moisture range from 0-100% WFPS, more varied soil types from different locations and longer incubation periods (>30 days incubation). This will allow for more reliable and comparative data to obtain clearer results that could more authoritatively point to the greenhouse gas sequestration potentials of biochars.